Neurobiology of Disease 124 (2019) 489–504

Contents lists available at ScienceDirect

Neurobiology of Disease

journal homepage: www.elsevier.com/locate/ynbdi

Pridopidine stabilizes mushroom spines in mouse models of Alzheimer's disease by acting on the sigma-1 receptor

Daniel Ryskamp[a], Lili Wu[a], Jun Wu[a], Dabin Kim[b], Gerhard Rammes[b], Michal Geva[c,1], Michael Hayden[c,1], Ilya Bezprozvanny[a,d,*]

[a] Department of Physiology, University of Texas Southwestern Medical Center, Dallas, TX 75390, USA
[b] Department of Anesthesiology and Intensive Care, Technische Universität München, Munich 81675, Germany
[c] Prilenia Therapeutics, Herzliya, Israel
[d] Laboratory of Molecular Neurodegeneration, Peter the Great St. Petersburg Polytechnic University, St. Petersburg, Russia

ARTICLE INFO

Keywords:
3-PPP
Alzheimer's disease
APP knock-in mice
Calcium dysregulation
Mushroom spines
Presenilin-1-M146 V knock-in mice
Pridopidine
Sigma-1 receptor
Synaptic instability
Synaptoprotection

ABSTRACT

There is evidence that cognitive decline in Alzheimer's disease (AD) results from deficiencies in synaptic communication (e.g., loss of mushroom-shaped 'memory spines') and neurodegenerative processes. This might be treated with sigma-1 receptor (S1R) agonists, which are broadly neuroprotective and modulate synaptic plasticity. For example, we previously found that the mixed muscarinic/S1R agonist AF710B prevents mushroom spine loss in hippocampal cultures from APP knock-in (APP-KI) and presenilin-1-M146 V knock-in (PS1-KI) mice. We also found that the "dopaminergic stabilizer" pridopidine (structurally similar to the S1R agonist R(+)-3-PPP), is a high-affinity S1R agonist and is synaptoprotective in a mouse model of Huntington disease. Here we tested whether pridopidine and R(+)-3-PPP are synaptoprotective in models of AD and whether this requires S1R. We also examined the effects of pridopidine on long-term potentiation (LTP), endoplasmic reticulum calcium and neuronal store-operated calcium entry (nSOC) in spines, all of which are dysregulated in AD, contributing to synaptic pathology. We report here that pridopidine and 3-PPP protect mushroom spines from $A\beta_{42}$ oligomer toxicity in primary WT hippocampal cultures from mice. Pridopidine also reversed LTP defects in hippocampal slices resulting from application of $A\beta_{42}$ oligomers. Pridopidine and 3-PPP rescued mushroom spines in hippocampal cultures from APP-KI and PS1-KI mice. S1R knockdown from lenti-viral shRNA expression destabilized WT mushroom spines and prevented the synaptoprotective effects of pridopidine in PS1-KI cultures. Knockout of PS1/2 destabilized mushroom spines and pridopidine was unable to prevent this. Pridopidine lowered endoplasmic reticulum calcium levels in WT, PS1-KO, PS1-KI and PS2 KO neurons, but not in PS1/2 KO neurons. S1R was required for pridopidine to enhance spine nSOC in PS1-KI neurons. Pridopidine was unable to rescue PS1-KI mushroom spines during pharmacological or genetic inhibition of nSOC. Oral pridopidine treatment rescued mushroom spines *in vivo* in aged PS1-KI-GFP mice. Pridopidine stabilizes mushroom spines in mouse models of AD and this requires S1R, endoplasmic reticulum calcium leakage through PS1/2 and nSOC. Thus, pridopidine may be useful to explore for the treatment of AD.

1. Introduction

Alzheimer's disease (AD) undermines cognitive functioning through progressive impairment of synaptic connections and neuronal atrophy (Selkoe, 2002). It is the most prevalent cause of dementia and the sixth leading cause of death in the United States (Alzheimer's's, 2015). It

Abbreviations: 3-PPP, R(+)-3-(3-hydroxyphenyl)-N-propylpiperidine; Aβ, amyloid-β; ACSF, artificial cerebrospinal fluid; AD, Alzheimer's disease; ADDLs, $A\beta_{1-42}$-derived diffusible ligands; APP, amyloid precursor proteins; APP-KI, APP knock-in; DIV, day *in vitro*; ER, endoplasmic reticulum; FAD, familial AD; GFP, green fluorescent protein; hS1R, human sigma-1 receptor; KO, knockout; LacZ, β-galactosidase; LTP, long-term potentiation; M1R, muscarinic acetylcholine receptor M1; NLS, nuclear localization sequence; nSOC, neuronal store-operated calcium entry; PEI, polyethylenimine; PFA, paraformaldehyde; PS1, presenilin-1; PS1-KI, presenilin-1-M146V knock-in; PS2, presenilin-2; S1R, sigma-1 receptor; shS1R, anti-S1R shRNA; STIM1, stromal interaction molecule 1; STIM2, stromal interaction molecule 2; Tg, thapsigargin; WT, wild type

* Corresponding author at: 5323 Harry Hines Blvd., ND12.200, Dallas, TX 75390, USA.
E-mail addresses: g.rammes@tum.de (G. Rammes), Ilya.Bezprozvanny@UTSouthwestern.edu (I. Bezprozvanny).
[1] Michal Geva and Michael Hayden are formerly affiliated with Teva Pharmaceutical Industries, Ltd, 5 Basel St., Petach Tikva, 49131, Israel.

https://doi.org/10.1016/j.nbd.2018.12.022
Received 14 September 2018; Received in revised form 12 November 2018; Accepted 26 December 2018
Available online 27 December 2018
0969-9961/

afflicted approximately 6 million Americans as of 2017 and its prevalence is expected to drastically increase over the coming decades (Brookmeyer et al., 2018). The risk of developing AD escalates with age or harboring certain alleles (e.g., APOE ε4) (Saunders et al., 1993). Although the vast majority of AD cases are considered sporadic, < 1% are caused by autosomal dominant mutations in proteins such as amyloid precursor protein (APP), presenilin-1 (PS1) or presenilin-2 (PS2) (Van Cauwenberghe et al., 2016). AD pathology involves aberrant changes in neurophysiology (e.g., dysregulation of calcium signaling, oxidative stress, mitochondria dysfunction), inflammation, accumulation of amyloid-β plaques and aggregation of neurofibrillary tangles of hyperphosphorylated tau protein (Kumar and Singh, 2015; Ryskamp et al., 2016). These factors conspire to weaken synaptic connections, impairing long-term memory storage (Ryskamp et al., 2016; Selkoe, 2002; Tackenberg et al., 2009). As thin spines convert into mushroom spines during information storage and in response to LTP (Bourne and Harris, 2007; Hayashi-Takagi et al., 2015), mushroom spine deficiency may reflect learning and memory defects in models of AD. Indeed, in both PS1-KI and APP-KI models of AD, hippocampal neuron mushroom spines are lost *in vitro* and *in vivo* (Sun et al., 2014; Zhang et al., 2015). Thus, drugs that stabilize mushroom spines could potentially stave off memory impairment in AD.

S1R is a transmembrane protein of 223 amino acids residing in the endoplasmic reticulum (ER) where it acts as a chaperone, modulating the activity of several client proteins of which several are ion channels (Kourrich et al., 2012). Although S1R was previously thought to have two transmembrane domains (Brune et al., 2014; Ortega-Roldan et al., 2015), a recent crystal structure suggested it might have only a single transmembrane domain (Schmidt et al., 2016). In addition to its role in neuromodulation (Maurice et al., 2006), S1R regulates neuroplasticity (Kourrich et al., 2012; Takebayashi et al., 2004; Tsai et al., 2009). For example, knockdown of S1R in hippocampal neurons causes shrinkage of spines (Tsai et al., 2009), whereas stimulation of S1R activity promotes hippocampal long-term potentiation and neurogenesis (Moriguchi et al., 2013). This is of interest in the context of AD because the density of S1R binding-sites is reduced early in AD in the cortex, hippocampus and other brain regions (Jansen et al., 1993; Mishina et al., 2008). Interestingly, common genetic variants of S1R may modify risk of AD in carriers of the APOE ε4 allele (Fehér et al., 2012; Huang et al., 2011; Maruszak et al., 2007; Uchida et al., 2005). S1R agonists have anti-amnestic properties, rescuing learning and memory impairments from scopolamine or amyloid-β toxicity (Maurice and Goguadze, 2017). S1R agonists also modulate several neuroprotective pathways and have demonstrated preclinical efficacy in animal models of AD. For example, the mixed muscarinic/S1R agonist AF710B stabilized mature mushroom spines *in vitro* in hippocampal cultures prepared from AD mice (PS1-KI and APP-KI models) and *in vivo* treatment of 3xTg-AD mice with AF710B reduced levels of BACE1, $A\beta_{1-42}$, plaques, p25/CDK5, GSK-3β activity, Tau phosphorylation and memory deficiency in the Morris water-maze (Fisher et al., 2016). AF710B was also disease-modifying in McGill-R-Thy1-APP transgenic rats, reducing amyloid burden and inflammation while enhancing synaptogenesis and cognition (Hall et al., 2017).

Several other S1R agonists including PRE-084, (−)-MR22, ANAVEX1–41, ANAVEX2–73, DHEA, and pregnenolone sulfate treat the hallmarks of AD *in vivo* following injection of $A\beta_{25-35}$ into the CNS of rodents by reducing $A\beta_{1-42}$, GSK-3β activity, hyperphosphorylated Tau, neuroinflammation, oxidative stress, endoplasmic reticulum (ER) stress, apoptosis of hippocampal neurons and memory impairments (Maurice and Goguadze, 2017; Meunier et al., 2006). Also, the acetylcholine esterase inhibitor donepezil, which is approved for use in the treatment of AD, is a high affinity S1R agonist and its anti-amnestic and neuroprotective properties may be partially mediated by S1R (Meunier et al., 2006). In APP_{Swe} AD mice knockout of S1R increases oxidative stress in the hippocampus and promotes memory deficits (Maurice and Goguadze, 2017; Maurice et al., 2018). These and other examples (Mancuso et al., 2012; Maurice and Lockhart, 1997; Mavlyutov et al., 2013; Mavlyutov et al., 2011; Nakazawa et al., 1998; Ono et al., 2014; Ryskamp et al., 2017; Smith et al., 2008) show that S1R agonists are broadly neuroprotective and loss of S1R worsens neurodegenerative phenotypes.

Pridopidine (a.k.a. ACR16, ASP2314 or Huntexil) was originally classified as a "dopaminergic stabilizer" due to its ability to increase locomotion in hypoactive rodents and decrease locomotion in hyperactive rodents, which was thought to result from modulation of dopaminergic tone via low-affinity regulation of dopamine receptor D_2 (Rung et al., 2008). More recent studies demonstrated that pridopidine acts as a high-affinity S1R ligand (Sahlholm et al., 2013). In previous studies we demonstrated that pridopidine is synaptoprotective in a mouse model of Huntington disease, behaving as an S1R agonist (Ryskamp et al., 2017). We further demonstrated that pridopidine activates neuroprotective pathways impaired in HD and improves behavioural and transcriptional deficits in HD mice (Garcia-Miralles et al., 2017; Geva et al., 2016; Kusko et al., 2018). Consistent with these findings, pridopidine has demonstrated promising results in human HD trials (de Yebenes et al., 2011; Esmaeilzadeh et al., 2011; Huntington Study Group, 2013; Lundin et al., 2010). In the present study, we tested whether pridopidine is synaptoprotective in models of AD and whether these effects require S1R. We also investigated the importance of modulating calcium signaling in the synaptoprotective actions of pridopidine.

2. Materials and methods

2.1. Mice

Experiments with mice were permitted by the Institutional Animal Care and Use Committee of the University of Texas Southwestern Medical Center at Dallas and followed the National Institutes of Health Guidelines for the Care and Use of Experimental Animals. Wild type (WT; C57/B6J), presenilin-1-M146 V knock-in (PS1-KI) (Guo et al., 1999), conditional presenilin double-knockout mice ($PS1^{flox/flox}$, $PS2^{-/-}$) (Zhang et al., 2010) and amyloid precursor protein knock-in (APP-KI; a.k.a. App^{NL-F}) mice harboring Swedish (KM670/671NL) and Beyreuther/Iberian (I716F) mutations in the APP gene (Saito et al., 2014; Zhang et al., 2015) were kindly provided by Dr. Saido (Riken, Japan) and were housed in a barrier facility (12 h light/dark cycle) at UT Southwestern Medical Center. *thy1*-GFP line M mice (WT-GFP) (Feng et al., 2000) were crossed to PS1-KI mice to generate PS1-KI-GFP mice as we previously described (Zhang et al., 2016). PS1-KI and APP-KI mice were bred as homozygotes and WT-GFP and PS1-KI-GFP mice were heterozygous for the GFP allele. Both male and female mice were included in the study and, as no differences from gender were noted, data was pooled.

2.2. Preparation of hippocampal cultures and in vitro mushroom spine loss assay

To study hippocampal mushroom spine loss *in vitro*, hippocampal cultures were prepared from WT, PS1-KI, and APP-KI mice as in (Sun et al., 2014). 24 well plates with coverslips were prepared as follows. 12 mm glass coverslips were washed with 100% acetone, 100% ethanol and then 70% ethanol and separated onto clean paper towels with forceps and left to dry. They were then placed in wells of 24 well plates and exposed overnight (with the lid off) to UV light. These were wrapped in aluminum foil and stored until use. Just before harvesting hippocampi, coverslips were coated with poly-D-lysine coated (0.5 ml/well of 0.1 mg/ml poly-D-lysine in PBS for 30 min at 37 °C). Then postnatal day 0–1 pups were anesthetized on ice and decapitated with sharp scissors. Brains were removing following linear cuts of the scalp and skull across the midline and placed in ice cold dissection media (1 × Hank's Balanced Salt Solution, 16.36 mM HEPES, 10 mM $NaHCO_3$,

1 × penicillin-streptomycin) in medium petri dishes and hippocampi were isolated by dissection and surface vasculature was removed. Hippocampi were cut into ~500 μm chunks, poured into 50 ml Falcon tubes, centrifuged (800 rpm for 4 min), digested with papain dissolved in NeurobasalA medium (30 min at 37 °C in 500 μl of 114 U papain/10 ml NBA; Worthington), rinsed and centrifuged (2000 rpm for 4 min; Neurobasal-A medium (NBA) with 10% FBS and 25 μg/ml DNAse I), mechanically dissociated (by trituration in 500 μl of dissection media with 5 mg/ml DNAse I), rinsed by adding dissection media and centrifuging (2000 rpm for 4 min) and rinsed again by replacing dissection media with plating media (NBA, 1% FBS, 2% B27 and 0.5 mM L-glutamine) and centrifuging (2000 rpm for 4 min). The supernatant was aspirated and 2 ml of plating media was added to each Falcon tube per 24 wells to be plated. Hippocampal pellets were dissociated by gentle trituration with a 1 ml pipette and 80 μl of the cellular suspension was added to the top of each coverslip for 7 min before increasing the volume of plating media to 1 ml. Hippocampi from 5 to 6 brains were used to plate 24 wells of a 24-well plate. During the process of preparing the cell suspension, 24 well plates were removed from the incubator and poly-D-lysine was aspirated. Wells were rinsed with dissection media and then with plating media. After removing the media, a plastic pipette tip was used to position each coverslip in the centre of each well and any media squeezed out from under each coverslip was aspirated. The lid was left off to dry out remaining media until plating. This technique keeps the cell suspension confined to the surface of the coverslip, which is important for achieving the desired cellular density. Cells were maintained at 37 °C in a 5% CO_2 incubator. For fura-2 experiments, cells were feed weekly by addition of 500 μl of NBA, 2% B27 and 0.5 mM L-glutamine. For morphological analysis of spines based on TdTomato fluorescence or GCaMP5G imaging experiments, cultures were transfected on DIV7 with a high calcium phosphate technique (Jiang and Chen, 2006; Sun et al., 2014). Transfected cultures were fed on DIV14 with 500 μl of NBA, 2% B27 and 0.5 mM L-glutamine. When adding drugs to the cultures, drugs were diluted with NBA from 10 mM stock solutions (in DMSO). The drugs or the vehicle were then added to the wells. Starting on DIV15–17 for spine analyses or DIV13–15 for calcium imaging, cultures were treated with pridopidine or R(+)-3-PPP at (100 nM or 1 μM).

For analysis of spine morphology, cultures were fixed after 16 h of drug incubation. When treating with multiple drugs, they were added together. For fixation, media was removed and 500 μl of cold 4% formaldehyde plus 4% sucrose in PBS (pH 7.4) was added to each well. The plate was placed at 4 °C for 20 min and then wells were washed twice (10 min each) with cold PBS. A drop of Aqua-Poly/Mount (Polysciences, Inc.) was added to a microscope slide before transferring the coverslip using fine tip forceps. Slides were allowed to dry overnight before imaging. Spines were imaged using a 63 × glycerol objective (N.A. 1.3) on a confocal microscope (Leica SP5) with the pinhole set to one airy unit. *Z*-stacks were captured with a set size of 0.5 μm. Spine type abundance in one to three dendritic segments / neuron (~70–90 μm) was automatically scored using the NeuronStudio software package (Rodriguez et al., 2008) with manual correction while blinded to the condition. Spine shapes were categorized as described in (Sun et al., 2014), using the following cutoff values: aspect ratio for thin spines (AR_thin(crit)) = 2.5, head to neck ratio (HNR(crit)) = 1.3, and head diameter (HD(crit)) = 0.45 μm. Data were analyzed from at least three batches of cultures for each experiment.

2.3. Preparation of toxic Aβ oligomers

$A\beta_{1–42}$ was obtained from California Peptide and $A\beta_{1–42}$-derived diffusible ligands (ADDLs) were prepared as in (De Felice et al., 2007). In brief, $A\beta_{1–42}$ was aliquoted and dried in hexafluoro-2-propanol and stored until use at −80 °C. Undiluted, sterile Me_2SO_4 was added to an aliquot to make a 5 mM solution of $A\beta_{1–42}$. This was diluted to 100 μM in Ham's F-12 medium without glutamine (BioSource) and incubated overnight (4 °C). The solution was then centrifuged at 14,000 × *g* for 10 min (4 °C) to discard insoluble aggregates (protofibrils and fibrils). The supernatant, which contained soluble $A\beta_{1–42}$ ADDLs, was added on DIV15 to WT hippocampal cultures for 48 h, and then cells were fixed for spine analysis. The concentration of ADDLs was estimated based on the initial amount of $A\beta_{1–42}$ peptides.

For LTP experiments, $A\beta_{1–42}$ (order number H-1368; Bachem, CH-Bubendorf) was suspended in 100% HFIP (Sigma Aldrich) to approximately 1 mg/400 μl HFIP and shaken at 37 °C for 1.5 h. The HFIP was removed by evaporation using a Speedvac for approximately 30 min, and when completely dry, aliquots of 100 μg $A\beta_{1–42}$ were stored at −20 °C. The $A\beta_{1–42}$ was dissolved in DMSO (Sigma Aldrich) to a concentration of 100 μM with the aid of an ultrasonic water bath.

2.4. Brain slice preparation and field excitatory postsynaptic potentials (fEPSPs) recording

Transverse hippocampal slices (350 μm thick) were obtained from adult (2 month) mice that were isoflurane-anesthetized and decapitated. The experimental protocols were approved by the Ethical Committee on Animal Care and Use of the Government of Bavaria, Germany. The brain was rapidly removed, and slices were prepared in ice-cold Ringer solution using a vibroslicer (HM650V, Microm International, Walldorf, Germany). All slices were placed in a holding chamber for at least 60 min and were then transferred to a superfusing chamber for extracellular or whole-cell recordings. The flow rate of the solution through the chamber was 4 ml/min. The composition of the solution was 124 mM NaCl, 3 mM KCl, 26 mM $NaHCO_3$, 2 mM $CaCl_2$, 1 mM $MgSO_4$, 10 mM D-glucose, and 1.25 mM NaH_2PO_4, bubbled with a 95% O_2 / 5% CO_2 mixture, and had a final pH of 7.3. All experiments were performed at room temperature. $A\beta_{1–42}$ stock solution in DMSO was added to the bath solution to give a final $A\beta_{1–42}$ concentration of 50 nM.

Extracellular recordings of fEPSPs were obtained from the dendritic region of the CA1 region of the hippocampus using glass micropipettes (1–2 MΩ) filled with superfusion solution. Steady baseline recordings were made for at least 30 min before application of tetanic stimuli. For LTP induction, high-frequency stimulation conditioning pulses (100 pulses @ 100 Hz; 4–5 V) were applied to the Schaffer collateral–commissural pathway via two independent inputs. Pridopidine was applied via the bath solution for one hour before induction of LTP in one input. After 60 min of stable LTP $A\beta_{1–42}$ has been applied for 90 min and LTP has been induced in the other input.

Amplified fEPSPs were filtered (3 kHz), digitized (15 kHz) and measured and plotted online, using the "LTP-program" software (Anderson and Collingridge, 2001); available from http://www/ltp-program.com. Measurements of the slope of the fEPSP were taken between 20 and 80% of the peak amplitude. Slopes of fEPSPs were normalized with respect to the 20-min control period before tetanic stimulation.

2.5. Lenti-virus preparation

We used produced lenti-viruses to infect neurons and express nuclear localization sequence-green fluorescent protein (NLS-GFP), NLS-GFP-Cre, Cas9 and sgRNA. For NLS-GFP and NLS-GFP-Cre we used a lenti-expression vector (FUGW; addgene.org/14883/). We obtained lenti-Cas9-Blast (addgene.org/52962/) and lenti-GuidePuro (addgene.org/52963/) for CRISPR experiments. Lenti-viruses were produced by transfecting HEK293T cells with the plasmid of interest and lenti-viral production and packaging plasmids (Δ8.9 and VSVG). These were mixed in 1 ml of DMEM and 60 μl polyethylenimine (PEI) for 20 min (RT). Culture media (DMEM +10% FBS) was exchanged with 11.5 ml of NBA and the transfection mixture was added dropwise around the dish. Media was harvested 48 h later, centrifuged (2000 RPM for 5 min), filtered (0.45 μm pore size) and aliquoted into cryotubes, which were frozen in liquid nitrogen and stored at −80 °C until use. A total volume of 100 μl of lenti-virus media was added to each well on DIV7.

These lenti-viruses exhibited selective neuronal tropism as revealed by GFP expression and MAP2 immunostaining, with a ~90% neuronal transfection rate (Wu et al., 2016).

2.6. S1R knockdown and overexpression

S1R was knocked down using lenti-virus-mediated shRNA expression in hippocampal neurons. Plasmids encoding MISSION® shRNA targeting mouse S1R (clone ID: NM_011014.2-1138s21c1; sequence: CCGGCCTG TAGTAATCTCTGGTGAACTCGAGTTCACCAGAGATTACTACAGGTTT TTG) or scrambled shRNA were from Sigma-Aldrich (St. Louis, Mo., USA). For overexpression of S1R, cDNA for the human S1R (www.ncbi.nlm.nih.gov/nuccore/NM_005866.3) was subcloned into the lenti-viral vector using *Eco*RI and BamHI restriction sites. Plasmids were produced and purified using a Maxi-prep (NucleoBond Xtra kit; Macherey-Nagel), sequenced and lenti-viruses were prepared as described above. 100 µl of the collected lenti-virus media was added to each well of neuron cultures on DIV7. Functional analyses in the mushroom spine loss assay and nSOC imaging assay as well as prior Western blotting experiments (Fisher et al., 2016) validated the efficacy of the constructs.

2.7. CRISPR/Cas9-mediated deletion of PS1, STIM1 and STIM2

To delete neuronal presenilin-1 (PS1), stromal interaction molecule 1 (STIM1) and/or (STIM2) in hippocampal cultures we used the CRISPR/Cas9 system. sgRNA sequences targeting mouse STIM1 or STIM2 were designed using bioinformatics tools (crispr.mit.edu for predicted specificity and http://www.broadinstitute.org/rnai/public/analysis-tools/sgrna-design for predicted efficacy) and sgRNA plasmids targeting PS1 (gPS1), STIM1 (gSTIM1) or STIM2 (gSTIM2) were generated. A sgRNA sequence targeting the second coding exon of PS1 (GACGACCCCAGGGTAACTCCCGG) or the first coding exon of STIM1 (GAATACAGGAGCTAGCTCCG) or STIM2 (GTCGGGATCGGCCGGAG CGG) was subcloned into the lentiGuide-Puro plasmid (addgene.org/52963/) as in (Sanjana et al., 2014) following their target guide sequence cloning protocol (media.addgene.org/data/plasmids/52/52963/52963-attachment_IPB7ZL_hJcbm.pdf). The lenti-Cas9-Blast plasmid (addgene.org/52962/) was used to express Cas9. The efficacy of this approach was confirmed in (Wu et al., 2016). As in (Platt et al., 2014), sgRNA (GTGCGAATACGCCCACGCGAT) targeting the bacterial gene β-galactosidase (LacZ) was used as a negative control (gLacZ). Functional analysis in the mushroom spine loss assay as well as prior Western blotting experiments (Wu et al., 2018; Wu et al., 2016) validated the efficacy of the approach and constructs.

2.8. Fura-2 calcium imaging

Cytosolic calcium was imaged using Fura-2 as described (Sun et al., 2014) on DIV14–16. Hippocampal cultures were loaded with Fura-2-AM (5 µM; Molecular Probes) in the presence of pluronic acid for 45 min at 37 °C and transferred to a recording chamber filled with artificial cerebrospinal fluid (ACSF) (140 mM NaCl, 10 mM HEPES, 5 mM KCl, 2 mM $CaCl_2$ and 1 mM $MgCl_2$, with the pH set to 7.3). Fura-2 was excited with 340 and 380 nm light from a DeltaRAM-X illuminator and 510 nm emissions were detected with an Evolve camera and Easy-RatioPro software (Photon Technology International, Inc.). Calcium levels were monitored via the ratio of emissions evoked by 340 nm and 380 nm light (340F/380F ratio). To measure the concentration of calcium in ionomycin-sensitive calcium pool, calcium-containing ACSF was replaced with calcium-free ACSF (containing 100 µM EGTA) 30 s prior to the application of 5 µM IO and the calcium signals were recorded as R = 340F/380F. The size of the ER calcium pool was estimated by integrating the area under the response curve as described (Wu et al., 2016). Hippocampal neurons were distinguished from glia as in (Sun et al., 2014) by their distinctive morphology. Data were analyzed from at least three batches of cultures for each experiment.

2.9. GCaMP5G calcium imaging

Calcium in hippocampal neuron spines was imaged as previously described (Sun et al., 2014). On DIV7 hippocampal cultures were transfected with a plasmid encoding GCaMP5G (Jiang and Chen, 2006) using a high calcium phosphate method (CalPhos Transfection Kit; Clontech). Hippocampal neurons in the cultures were identified as in (Sun et al., 2014) by their characteristic morphology. GCaMP5 was excited with a Prior Lumen 200 illuminator (488 nm excitation) and imaged with an Olympus IX70 inverted epifluorescence microscope (60× lens) equipped with a Cascade 650 digital camera (Roper Scientific). Calcium signals were imaged at 0.5 Hz using MetaFluor imaging software (Universal Imaging). Neuronal store-operated calcium entry (nSOC) was measured by removing extracellular calcium (calcium free ACSF with 400 µM EGTA) and blocking the SERCA pump with 1 µM thapsigargin (Tg) for 10 min before replacing this solution with ACSF containing 2 mM calcium, 1 µM Tg and a calcium channel inhibitor cocktail (1 µM TTX, 50 µM AP5, 10 µM CNQX and 50 µM nifedipine). Baseline calcium (F0) in calcium-free media was imaged for 40 s prior to calcium re-addition. F = peak response from calcium add back. Calcium trace data was obtained using ImageJ (NIH) and mean intensity values were further analyzed in Microsoft Excel. Data were analyzed from at least three batches of cultures for each experiment.

2.10. Western blotting

Mice were euthanized (euthasol injection and cervical dislocation) and hippocampi were removed in PBS by dissection from WT and PS1-KI mice at 3, 6, and 12 months of age. For each hippocampus, 200 µl of cold lysis buffer (1% CHAPS, 137 mM NaCl, 2.7 mM KCl, 4.3 mM Na2HPO4, 1.4 mM KH2PO4, pH 7.2, 5 mM EDTA, 5 mM EGTA, 1 mM PMSF, 50 mM NaF, 1 mM Na3VO4 and protease inhibitors) was used to homogenize the tissue (by trituration) and solubilize protein (rotating at 4 °C for 1 h). After homogenates were centrifuged in 1.5 ml tubes at 10,000 g for 10 min at 4 °C, the supernatant was collected. The concentration of protein in each sample was measured with a NanoDrop. Enough 6× SDS sample buffer was added to each sample for a final concentration of 1×. As needed, samples were diluted with 1× SDS buffer to standardize protein concentrations across samples. Culture samples were prepared by lysing cells with 1× SDS buffer, followed by brief sonication. Samples were heated at 90 °C for 3 min, separated by SDS-PAGE and analyzed by Western blotting with mouse anti-S1R mAb (1:200–1:1000, Santa Cruz, sc-137,075), rabbit anti-sigma-2 receptor/TMEM97 pAb (1:2500; Novus Biologicals, NBP1–30436), mouse anti-dopamine D_2 receptor mAb (1:1000; Abcam, ab88074), mouse-anti-PS1 mAb (1:5000; Millipore, MAB5232) and mouse anti-tubulin mAb (1:5000, DSHB, E7-c). The HRP-conjugated anti-mouse (111-035-144) and anti-rabbit (115-035-146) secondary antibodies were from Jackson ImmunoResearch. Bands were analyzed with ImageJ by normalizing the density of each band to tubulin signal of the same sample.

2.11. In vivo hippocampal mushroom spine analysis

WT-GFP and PS1-KI-GFP mice were aged to 5 months of age and then treated daily for one month by mouth with 30 mg / kg or pridopidine dissolved in water. At six month of age, mice were exsanguinated and intracardially perfused with ice-cold PBS followed by freshly prepared 4% paraformaldehyde (PFA) in PBS, pH 7.4 (3 min each with the peristaltic pump perfusing 10 ml per min). The brains were removed and postfixed in 4% PFA in PBS overnight. 50 µm thick coronal slices were then made with a vibratome (Leica 1200S). GFP-positive CA1 pyramidal neurons were then imaged with a Leica SP5 (63× glycerol objective, N.A. 1.3). *Z*-stacks with a step size of 0.5 µm captured the second order apical dendrites. As described above and in (Rodriguez et al., 2008; Zhang et al., 2015), we used NeuronStudio to quantify the density of spines and classify them based on shape.

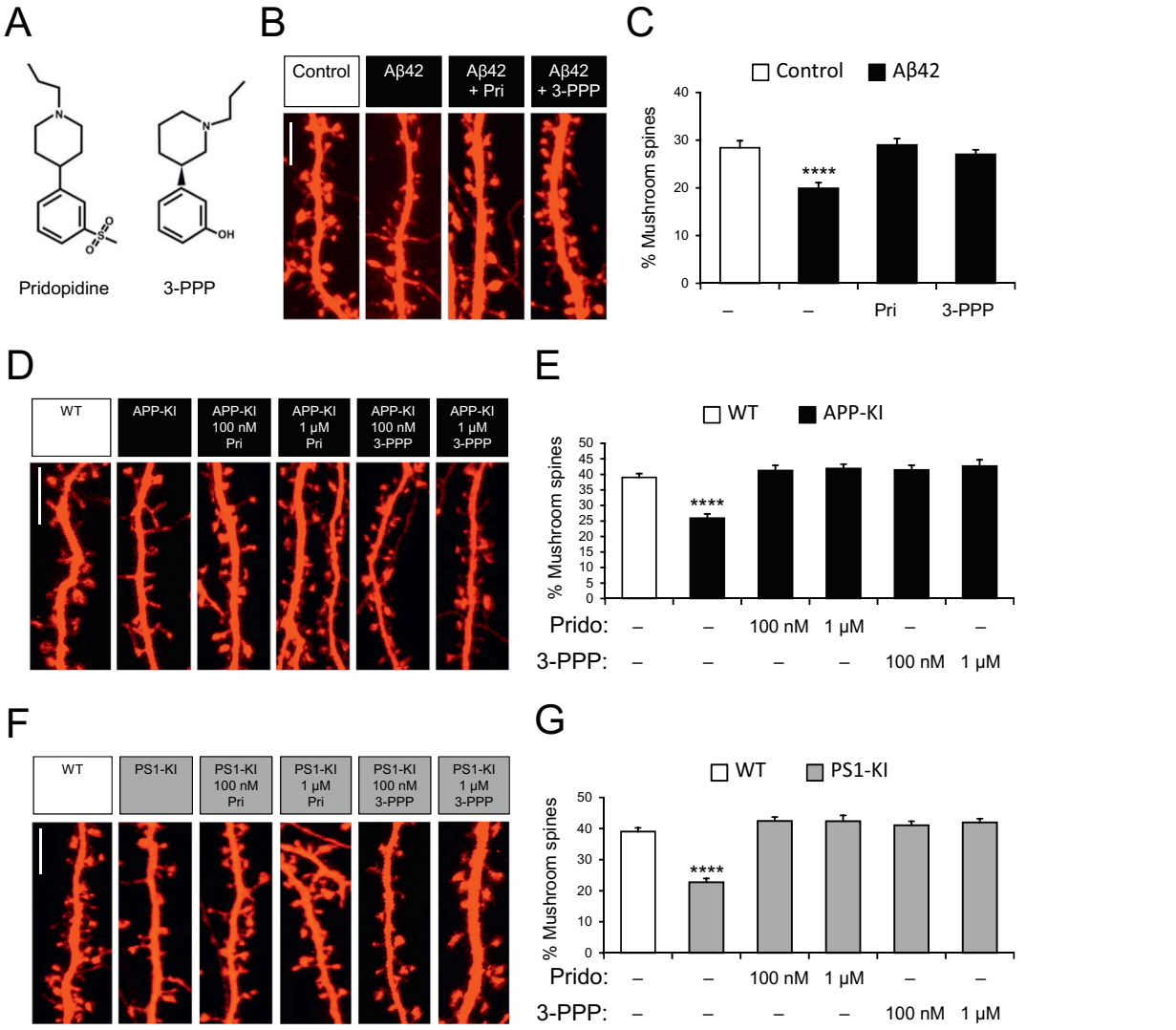

Fig. 1. Pridopidine and 3-PPP prevent loss of mushroom spines from $A\beta_{42}$ oligomer toxicity or AD mutations in hippocampal cultures. (A) Chemical structures of pridopidine and 3-PPP adapted from (Sahlholm et al., 2013). (B) Confocal images of dendrites and spines expressing TdTomato in WT hippocampal cultures. Scale bar = 5 μm. (C) Quantitative summary of mushrooms spine prevalence in WT hippocampal cultures treated for 48 h starting on DIV14–15 with vehicle or $A\beta_{42}$ ADDLs (5 μM) and for 16 h prior to fixation with the vehicle (n = 16 neurons for control and $A\beta_{42}$), 100 nM pridopidine (n = 15 neurons), or 100 nM 3-PPP (n = 16 neurons). (D) Confocal images of spines expressing TdTomato in WT and APP-KI hippocampal cultures. Scale bar = 5 μm. (E) Quantitative summary of mushrooms spine prevalence in WT (n = 13 neurons) and APP-KI hippocampal cultures treated for 16 h on DIV15–16 with the vehicle (n = 15 neurons), 100 nM pridopidine (n = 15 neurons), 1 μM pridopidine (n = 9 neurons), 100 nM 3-PPP (n = 12 neurons) or 1 μM 3-PPP (n = 12 neurons). (F) Confocal images of spines expressing TdTomato in WT and PS1-KI hippocampal cultures. Scale bar = 5 μm. (G) Quantitative summary of mushrooms spine prevalence in WT (n = 13 neurons) and PS1-KI hippocampal cultures treated for 16 h on DIV15–16 with the vehicle (n = 15 neurons), 100 nM pridopidine (n = 17 neurons), 1 μM pridopidine (n = 11 neurons), 100 nM 3-PPP (n = 15 neurons) or 1 μM 3-PPP (n = 13 neurons). Results are shown as mean ± S.E. Experimental conditions were compared to the WT control condition using the Holm-Bonferroni test. ****p < .0001.

2.12. Statistical analyses

Data are presented as mean ± standard error. Unpaired t-tests were used for single comparisons and the Holm-Bonferroni method was used for multiple comparisons as specified. α was set at 0.05. $p < 0.05$ = *, $p < 0.01$ = **, $p < 0.001$ = *** and $p < 0.0001$ = ****.

3. Results

3.1. S1R agonists prevent mushroom spine loss from Aβ toxicity or AD-causing mutations in hippocampal neuronal cultures

We previously demonstrated that incubating hippocampal cultures with $A\beta_{42}$ oligomers causes loss of mushroom spines (Popugaeva et al., 2015; Zhang et al., 2015). In our initial experiments we tested whether treatment with pridopidine (Fig. 1A) or the structurally similar S1R agonist 3-PPP (Fig. 1A) can prevent this. Primary hippocampal cultures were prepared from WT pups on postnatal day 0–1 and were transfected on day *in vitro* (DIV) 7 with a plasmid encoding TdTomato for later visualization of dendritic spine morphology. $A\beta_{42}$ was oligomerized to form synaptotoxic $A\beta_{42}$-derived diffusible ligands (ADDLs) as we previously described (Popugaeva et al., 2015; Zhang et al., 2015). The ADDLs were applied for 48 h (5 μM) to the cultures on DIV15. Cultures were then fixed and coverslips were prepared for imaging. Consistent with our previous findings (Popugaeva et al., 2015; Zhang et al., 2015), application of ADDLs reduced the fraction of spines that were classified as mushroom spines (Fig. 1B, C). A 16-h treatment with 100 nM pridopidine or 3-PPP prevented this reduction in the prevalence of mushroom spines (Fig. 1B, C). Similar results were obtained when we quantified the density of mushroom spines. On average for every 10 μm

of dendritic length there were 2.35 ± 0.20 mushroom spines in the control condition, 1.44 ± 0.16 mushroom spines in the $A\beta_{42}$ condition, 2.29 ± 0.21 mushroom spines in the $A\beta_{42}$ + 100 nM pridopidine condition and 2.22 ± 0.65 mushroom spines in the $A\beta_{42}$ + 100 nM 3-PPP condition. As the pattern of results was similar to when we quantified the relative prevalence of mushroom spines, we used the later type of analysis for the remainder of this study to remain consistent with our previous reports.

Mushroom spine loss from $A\beta_{42}$ accumulation is also observed in hippocampal cultures prepared from APP-KI mice and *in vivo* (Zhang et al., 2015). The concentration of $A\beta_{42}$, but not $A\beta_{40}$, is elevated in the media of hippocampal neuron cultures from APP-KI mice (Zhang et al., 2015). Consistent with these results, we discovered that the abundance of mushroom spines was reduced in APP-KI cultures compared to WT cultures (Fig. 1D, E). A 16 h incubation with 100 nM pridopidine, 1 μM pridopidine, 100 nM 3-PPP or 1 μM 3-PPP was sufficient to elevate the prevalence of APP-KI mushroom spines to WT levels (Fig. 1D, E).

We expanded our studies to the PS1-KI mouse model of familial AD (Guo et al., 1999). PS1-KI mice do not generate the synaptotoxic human $A\beta_{42}$ peptide, as they do not express human APP. We previously demonstrated that mushroom spine loss in these neurons is due to ER calcium signaling defects resulting from the PS1-M146 V mutation (Sun et al., 2014). As we have observed previously (Sun et al., 2014), the prevalence of mushroom spines was reduced in PS1-KI cultures compared to WT cultures (Fig. 1F, G). A 16-h incubation with 100 nM pridopidine, 1 μM pridopidine, 100 nM 3-PPP or 1 μM 3-PPP increased the fraction of PS1-KI mushroom spines to WT levels (Fig. 1F, G). These results indicate that pridopidine and 3-PPP protect against mushroom spine loss from amyloid toxicity and the M146 V mutation in PS1.

3.2. Pridopidine restores hippocampal LTP deficits induced by $A\beta_{42}$ oligomers

Long-term potentiation (LTP) causes spine volume to increase in CA1 hippocampal neurons (Bourne and Harris, 2007; Bromer et al., 2018) and LTP is impaired by $A\beta_{42}$ oligomer toxicity (Rammes et al., 2015; Rammes et al., 2011), possibly through dysregulation of glutamatergic and GABAergic signaling (Lei et al., 2016; Lublin and Gandy, 2010). We tested whether pridopidine can prevent deficits in LTP caused by $A\beta_{42}$ oligomer toxicity. In previous publications (Rammes et al., 2015; Rammes et al., 2011) we have demonstrated that application of synthetic $A\beta_{42}$ oligomers for 90 min to murine hippocampal slices prevents, in a concentration-dependent manner, the development of CA1-LTP after tetanic stimulation of the Schaffer collaterals with a half maximal inhibitory concentration of around 2 nM. In the present study, we tested whether pridopidine is able to restore LTP in the presence of such oligomeric $A\beta_{42}$ preparations. Under control conditions, 60 min after high frequency stimulation (HFS) delivery, fEPSPs were potentiated to 147.5% (n = 27), whereas after washing-in $A\beta_{42}$ (50 nM) for 90 min, the same stimulus produced a very small LTP (115.3%; n = 8; data not shown). We tested whether pridopidine at a concentration of either 30 nM or 100 nM is able to restore LTP in the presence of oligomeric $A\beta_{42}$. We discovered that both concentrations reversed the LTP deficits induced by 50 nM $A\beta_{42}$ (Fig. 2). Neither the application of $A\beta_{42}$ nor pridopidine affected fEPSPs *per se* (data not shown).

3.3. S1R is required for pridopidine to rescue mushroom spine loss in PS1-KI hippocampal neurons

Pridopidine and 3-PPP have a similar chemical structure and bind to S1R with a comparable affinity (Kd ~80 nM) (Sahlholm et al., 2013). Thus, although pridopidine was originally thought to stabilize dopaminergic signaling through partial inhibition of D2 receptors (Kd ~10 μM) (Dyhring et al., 2010; Nilsson et al., 2004; Rung et al., 2008), it's primary action at lower concentrations/doses is hypothesized to modulate S1R (Sahlholm et al., 2015). Indeed, we previously found that the synaptoprotective effects of pridopidine in HD striatal neurons require S1R (Ryskamp et al., 2017). We tested here whether S1R is required for the rescue of PS1-KI hippocampal mushroom spines by pridopidine.

To test the potential role of S1R in synaptoprotection from pridopidine and 3-PPP, we co-administered these agonists with the S1R antagonists NE-100, BD1047, or haloperidol (Fig. 3A). WT mushroom spines were unaffected by 100 nM pridopidine or 100 nM 3-PPP (Fig. 3A). However, application of S1R antagonists decreased the abundance of WT mushroom spines. When pridopidine and 3-PPP were applied together with S1R antagonists, they were unable to restore WT mushroom spines to normal levels (Fig. 3A). As before, pridopidine and 3-PPP rescued mushroom spines in PS1-KI cultures. S1R antagonists alone did not further destabilize mushroom spines in PS1-KI cultures; however, when applied together with pridopidine or 3-PPP, they blocked the rescue of mushroom spines (Fig. 3A). We previously found that AF710B also rescues PS1-KI mushroom spines and that it works through the combined activation of both muscarinic acetylcholine receptor M1 (M1R) and S1R (Fisher et al., 2016). Thus, we used the M1R antagonist pirenzepine to test whether M1R is required for the rescue of PS1-KI mushroom spines by pridopidine and 3-PPP (Fig. 3A). Application of 1 μM pirenzepine had no effect on WT or PS1-KI mushroom spines and it failed to block the rescue of PS1-KI mushroom spines by pridopidine and 3-PPP (Fig. 3A). These results indicate, that pridopidine and 3-PPP may stabilize PS1-KI spines through activation of S1R.

As pharmacological tools can engage additional targets, we further tested the synaptoprotective role of S1R using RNAi. To accomplish this, we infected hippocampal cultures with lenti-viruses encoding shRNA targeting mouse S1R mRNA (shS1R). We confirmed S1R knockdown in these cultures as we have previously reported (Fisher et al., 2016) and we verified that the expression of other potential targets of pridopidine (dopamine receptor D_2 and sigma-2 receptor/TMEM97) was not affected (data not shown). As we (Fisher et al., 2016) and others (Tsai et al., 2009) observed, knockdown of S1R in WT hippocampal neurons caused loss of mushroom spines (Fig. 3B, C). Knockdown of S1R in PS1-KI cultures did not further reduce the abundance of mushroom spines (Fig. 3B, C). Overexpression of human S1R rescued the mushroom spine loss phenotype associated with S1R knockdown in WT cultures, but was insufficient to rescue mushroom spines in PS1-KI cultures (Fig. 3B, C). As before (Fig. 1F, G), 100 nM pridopidine (16 h) had no effect on WT mushroom spines (Fig. 3B, C). Pridopidine was unable to stabilize mushroom spine loss associated with S1R knockdown in WT cultures (Fig. 3B, C). Also as before (Fig. 1E, F), pridopidine restored PS1-KI mushroom spines to WT levels; except when S1R was knocked down in PS1-KI cultures, pridopidine was rendered ineffective (Fig. 3B, C). Overexpression of human S1R (hS1R) restored the synaptoprotective properties of pridopidine in PS1-KI cultures without affecting the fraction of WT mushroom spines (Fig. 3B, C). Overexpression of human S1R (hS1R) was also unable to rescue mushroom spine loss in APP-KI cultures (APP-KI = 22.7 ± 2.2% + lenti-NLS-GFP, n = 6 vs. APP-KI + lenti-hS1R 21.6 ± 1.55%, n = 9; unpaired t-test, $p > .05$) (data not shown). Thus, background levels of S1R activity are needed for spine stability in WT neurons, but agonist-mediated activation of S1R is necessary to prevent spine loss in diseased neurons. These data are consistent with the possibility that S1R mediates the protective action of pridopidine and further indicates that pridopidine is an S1R agonist.

As S1R expression may be reduced in AD patients (Jansen et al., 1993; Mishina et al., 2008) and S1R knockdown destabilized mushroom spines (Fig. 3B, C), downregulation of S1R may contribute to AD pathology. Thus, we examined whether S1R is downregulated the hippocampus of PS1-KI mice. We euthanized WT and PS1-KI mice at 3, 6 and 12 months of age, isolated hippocampi and extracted protein. Hippocampal lysates were separated by SDS-PAGE and S1R protein expression was analyzed by Western blotting. We observed no

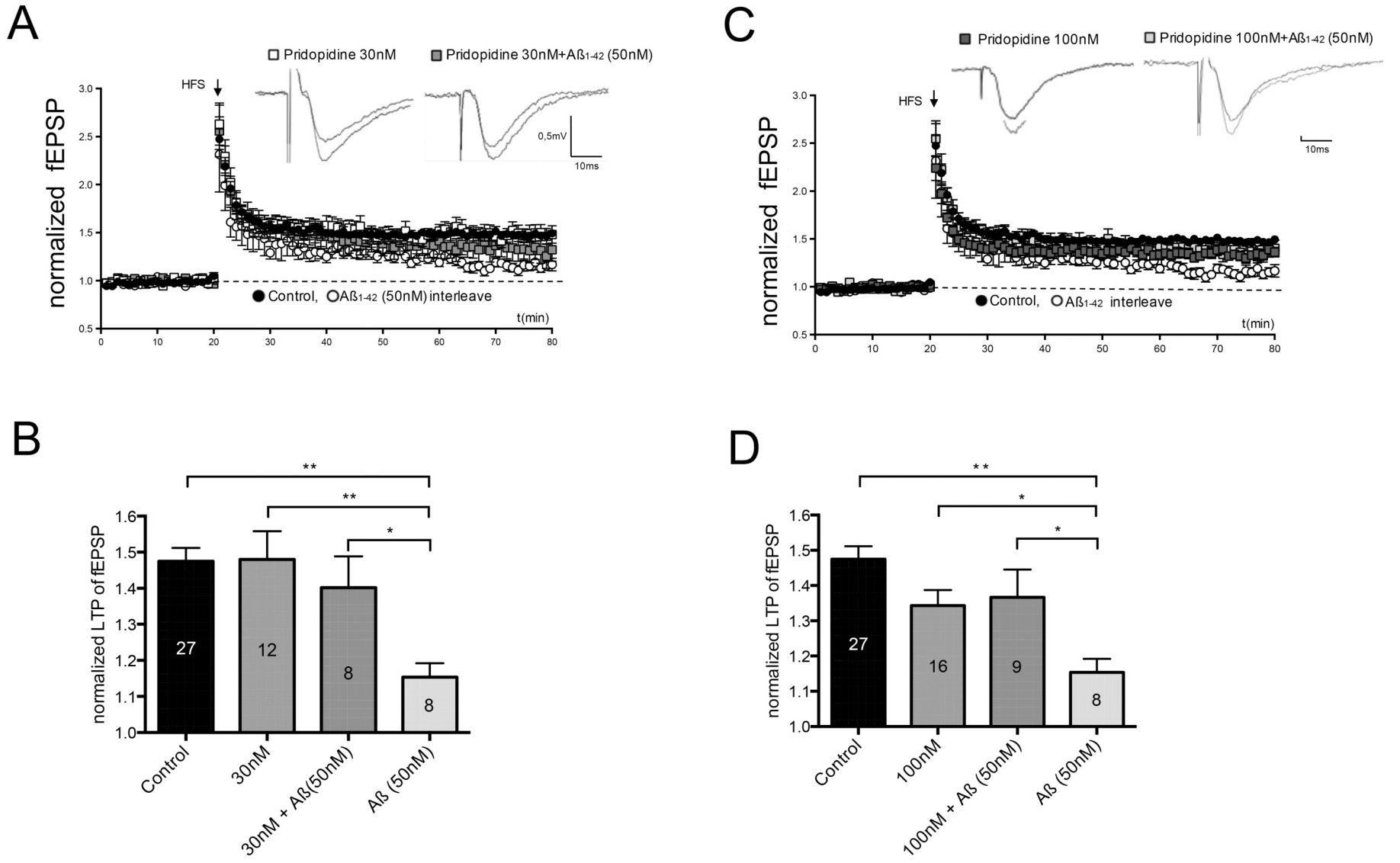

Fig. 2. Pridpopidine reverses $A\beta_{42}$-induced impairment of LTP in acute hippocampal slices.
(A) The slope of evoked hippocampal excitatory postsynaptic potentials (fEPSP) fEPSP was measured following incubation with 30 nM pridopidine (open squares, n = 12), 50 nM $A\beta_{42}$ (open circles, $n = 8$), or 30 nM pridopidine and 50 nM of $A\beta_{42}$ (gray squares, n = 8). HFS stimulation was applied as indicated by arrow. The insets show representative fEPSP traces before and after HFS. (B) The magnitude of LTP potentiation is shown as a percentage potentiation of the fEPSP slope values averaged from the last 10 min of the recordings for conditions as indicated. The values are displayed as means ± S.E.M. (C) The slope of fEPSP was measured following incubation with 100 nM pridopidine (dark squares, n = 16), 50 nM $A\beta_{42}$ (open circles, n = 8), or 100 nM pridopidine and 50 nM of $A\beta_{42}$ oligomers (light gray squares, $n = 9$). HFS stimulation was applied as indicated by arrow. The insets show representative fEPSP traces before and after HFS. (D) The magnitude of LTP potentiation is shown as a percentage potentiation of the fEPSP slope values averaged from the last 10 min of the recordings for conditions as indicated. The values are displayed as means ± S.E.M.

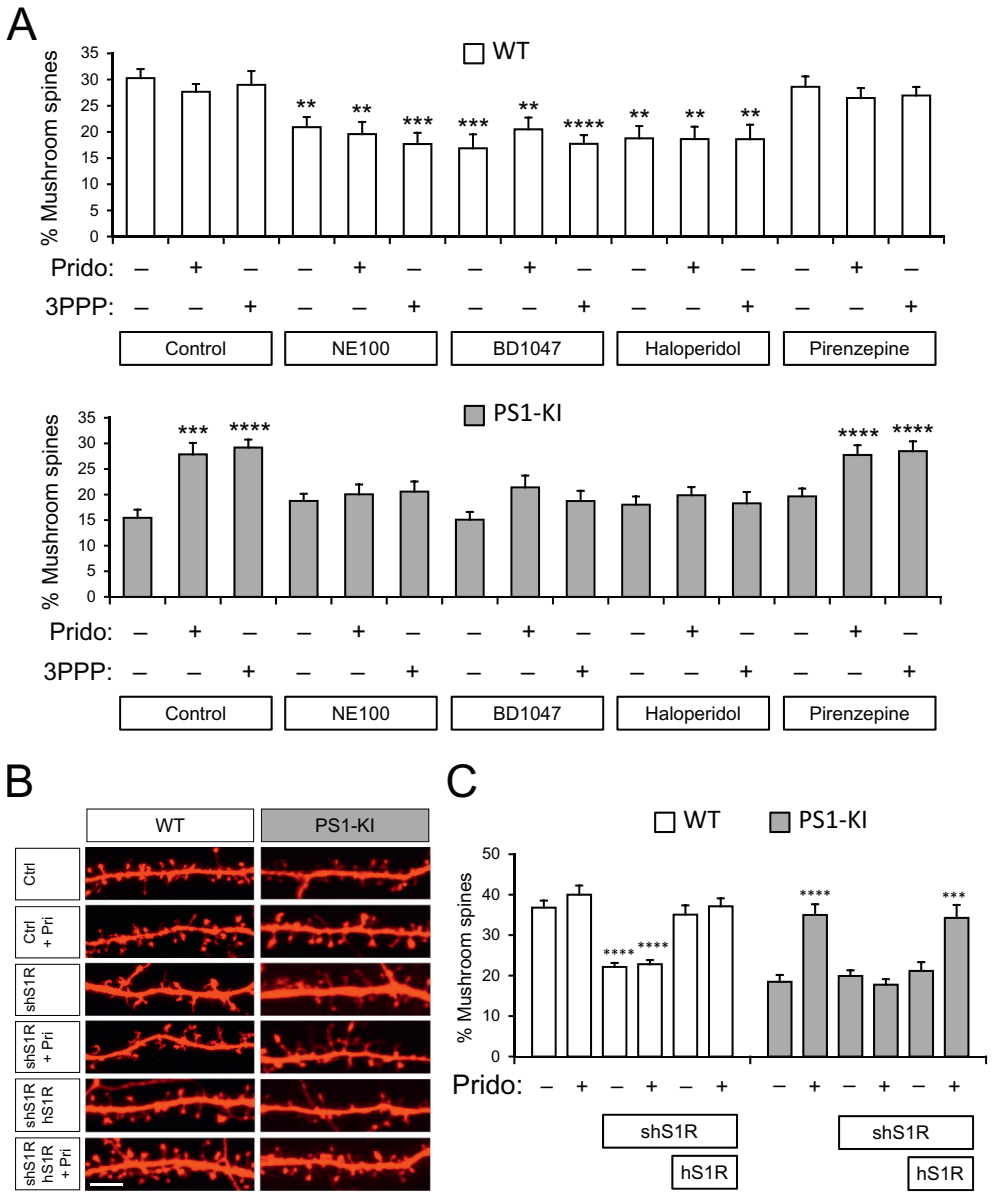

Fig. 3. S1R is required for pridopidine to rescue mushroom spine loss in PS1-KI hippocampal neurons. (A) Quantitative summary of mushrooms spine prevalence in WT and PS1-KI hippocampal cultures treated for 16 h on DIV16–17 with the vehicle, 100 nM pridopidine, 100 nM 3-PPP or 1 μM 3-PPP with or without 100 nM NE-100, 100 nM BD1047, 100 nM haloperidol or 1 μM pirenzepine. n = 9–10 neurons per condition for WT and 15 neurons per condition for PS1-KI. (B) Confocal images of spines expressing TdTomato in WT and PS1-KI hippocampal cultures infected on DIV7 with lenti-virus particles to encode scrambled shRNA, shRNA targeting S1R (shS1R) and/or human S1R (hS1R). Scale bar = 5 μm. (C) Quantitative summary of mushrooms spine prevalence in WT and PS1-KI hippocampal cultures treated for 16 h on DIV15–16 with the vehicle or 100 nM pridopidine. The number of analyzed neurons for WT was 15 for control, 12 for pridopidine, 13 for siS1R, 15 for siS1R + pridopidine, 12 for siS1R + hS1R and 12 for siS1R + hS1R + pridopidine. The number of analyzed neurons for PS1-KI was 12 for each condition. Mean ± S.E. Experimental conditions were compared to the control condition for each genotype using the Holm-Bonferroni test. **p < 0.01. ***p < 0.001. ****p < 0.0001.

significant changes in S1R expression between WT and PS1-KI mice at these ages (data not shown). Thus, mushroom spine loss from the PS1-KI mutation does not result from decreased S1R protein expression.

3.4. Pridopidine is able to correct mushroom spine loss in presenilin 1 or presenilin 2 knockout neurons, but not in PS1/2 double knockout neurons

There are 2 presenilin genes that can be mutated in familial AD (FAD) — PS1 and PS2. In previous studies we demonstrated that FAD mutations in either PS1 or PS2 affect ER Ca^{2+} signaling by disrupting tonic Ca^{2+} release from the ER via PS1 and PS2 leak channels (Tu et al., 2006b). We took a genetic approach to evaluate importance of PS1 and PS2 genes for stability of hippocampal mushroom spines. In these studies we took advantage of $PS1^{flox/flox}$, $PS2^{-/-}$ mice that were utilized in our previous work (Zhang et al., 2010). When compared to WT cultures, there was a trend toward mushroom spine loss in PS2 KO cultures (cultures from conditional presenilin double-knockout mice ($PS1^{flox/flox}$, $PS2^{-/-}$) infected with lenti-NLS-GFP on DIV7). The percentage of mushroom spines was non-significantly reduced in PS2 KO cultures (Fig. 4A, B). We also tested whether pridopidine was protective in this context. A 16-h treatment with 1 μM pridopidine had no effect on WT cultures, but elevated the fraction of PS2 KO mushroom spines to WT levels (Fig. 4A, B). Next, we examined spine morphology in the absence of both presenilin isoforms. In PS1/2 KO cultures ($PS1^{flox/flox}$, $PS2^{-/-}$ cultures infected with lenti-NLS-GFP-Cre on DIV7) the density of mushroom spines was significantly reduced compared to WT cultures (Fig. 4A, B). In PS1/2 KO cultures treated with pridopidine, mushroom spines remained sparse (Fig. 4A, B). We used the CRISPR/Cas9 system to impede PS1 expression. For this we infected hippocampal cultures on DIV7 with lenti-Cas9 and lenti-guideRNA. GuideRNA targeting the bacterial LacZ gene was used as a control (gLacZ) and guide RNA targeting the PS1 gene was used to ablate PS1 in neurons (gPS1). We confirmed the effectiveness of this approach using Western blotting (Fig. 4C). Some PS1 remained as our lenti-viral approach is selective for neurons (as indicated by selective and wide-spread neuronal tropism with lenti-GFP expression in our previous studies), leaving residual PS1 protein in glia. As expected, pridopidine had no effect on mushroom spines in gLacZ cultures (Fig. 4D, E). We observed a loss of mushroom spines in gPS1 cultures and 1 μM pridopidine prevented this loss (Fig. 4D, E). These results suggest that PS1 and perhaps PS2 perform a critical function for mushroom spine stability. In the absence of either PS1 or PS2, pridopidine can compensate and restore synaptic integrity.

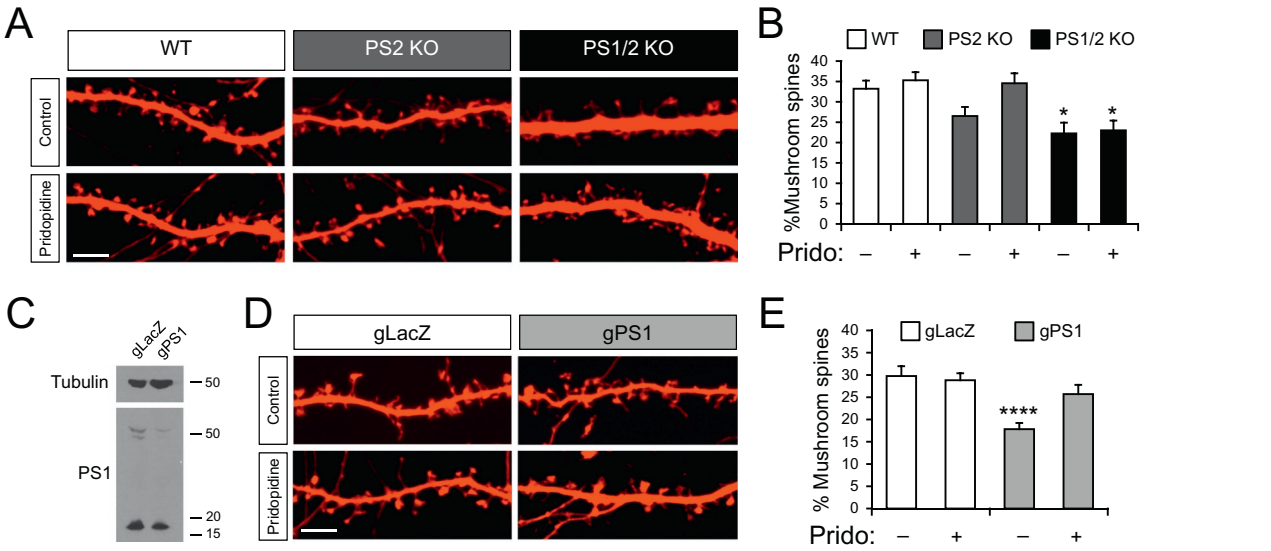

Fig. 4. Knockout of PS1/2 destabilizes mushroom spines and pridopidine is unable to rescue the spines. (A) Confocal images of spines expressing TdTomato in WT and PS2 KO/PS1$^{Flox/Flox}$ hippocampal cultures infected on DIV7 with lenti-virus particles to encode NLS-GFP (PS2 KO) or NLS-GFP-Cre (PS1/2 KO). Scale bar = 5 μm. (B) Quantitative summary of mushrooms spine prevalence in WT, PS2 KO and PS1/2 KO hippocampal cultures treated for 16 h on DIV15–16 with the vehicle or 1 μM pridopidine. n = 16 neurons for WT, 17 neurons for WT + pridopidine, 18 neurons for PS2KO, 16 neurons for PS2KO + pridopidine, 8 neurons for PS1/2KO and 8 neurons for PS1/2KO + pridopidine. (C) Western blot confirming a reduction in PS1 protein levels in hippocampal cultures infected on DIV7 with lenti-virus particles to encode Cas9 and guideRNA targeting the PS1 (gPS1) gene. guideRNA targeting the bacterial LacZ gene was used as a control (gLacZ). The upper bands around 50 kDa are the full-length PS1 holoprotein. The lower band at 17.5 kDa is the cleaved C-terminus of PS1. Residual PS1 in the gPS1 condition is likely from non-infected glial cells. (D) Confocal images of spines expressing TdTomato in WT hippocampal cultures infected on DIV7 with lenti-Cas9 and lenti-gLacZ or lenti-gPS1. Scale bar = 5 μm. (E) Quantitative summary of mushrooms spine prevalence in WT gLacZ and gPS1 hippocampal cultures treated for 16 h on DIV16 with the vehicle or 1 μM pridopidine. n = 9 neurons each for gLacZ conditions and 15 neurons each for gPS1 conditions. Experimental conditions were compared to the control condition using the Holm-Bonferroni test. *p < 0.05. ****p < 0.0001.

However, when both isoforms are knocked out, pridopidine is unable to overcome this deficit.

3.5. Pridopidine lowers ER calcium levels in hippocampal neurons, but not in PS1/2 KO hippocampal neurons

In addition to the role of cleaved PS1 in the γ-secretase complex, the holoprotein version of PS1 forms a leak channel in the ER membrane (Nelson et al., 2007; Tu et al., 2006a; Zhang et al., 2010). Likewise, PS2 holoprotein permits leakage of calcium ions from the ER lumen to the cytosol (Nelson et al., 2007; Tu et al., 2006a; Zhang et al., 2010). The absence of PS1 and PS2 would thus be expected to elevate the concentration of calcium in the ER (Zhang et al., 2010). As ER calcium homeostasis is crucial for synaptic maintenance (Sun et al., 2014; Zhang et al., 2016), we measured the effect of pridopidine on the concentration of ER calcium in WT, PS1-KI, PS2 KO and PS1/2 KO hippocampal neurons. To estimate ER calcium levels, hippocampal neurons were loaded with fura-2 and imaged. External calcium was removed and 30 s later 5 μM ionomycin was added to the recording chamber to release calcium from internal stores. The fura-2 ratio was recorded as calcium transited the cytoplasm on its way out of the cells and the area under the response curve was integrated to estimate the total amount of calcium that was released. Following 16–24 h of incubation with 1 μM pridopidine, ER calcium levels were significantly reduced in WT hippocampal neurons (Fig. 5A, B). This effect on ER calcium levels was also observed in SH-SY5Y neuroblastoma cells treated with 1 μM pridopidine for 3 h (vehicle-treated = 1 ± 0.093, $n = 122$ vs. pridopidine-treated = 0.404 ± 0.042, $n = 103$, unpaired-t-test, $p < .0001$) (data not shown). Compared to WT hippocampal neurons, ER calcium levels in PS1-KI and PS2 KO neurons were slightly, but non-significantly elevated (Fig. 5A, B). When both PS1 and PS2 were knocked out, ER calcium levels were significantly higher (Fig. 5A, B), as reported in our earlier studies (Zhang et al., 2010). The extent of ER calcium elevation in PS1/2 KO neurons was more than the extent of ER calcium elevation in PS1-KI and PS2 KO neurons combined, suggesting redundancy in the function of presenilin isoforms. When PS1-KI neurons were treated with 1 μM pridopidine (16–24 h), ER calcium levels were reduced approximately to levels in vehicle-treated WT neurons (Fig. 5A, B). Likewise, when PS2 KO neurons were treated with 1 μM pridopidine (16–24 h), ER calcium levels were also reduced (Fig. 5A, B). However, when both PS1 and PS2 were knocked out, pridopidine had no effect on the concentration of ER calcium (Fig. 5A, 5B). As in Fig. 4, we used the CRISPR/Cas9 system to ablate neuronal PS1. Similar to the results in Fig. 5A and B, pridopidine decreased ER calcium levels in Cas9/gLacZ-expressing cultures (Fig. 5C, D). Cas9/gPS1-expression slightly, but non-significantly increased the size of the ionomycin-releasable pool (Fig. 5C, D). Cas9/gPS1-expression did not prevent the reduction in ER calcium from pridopidine treatment (Fig. 5C, D). These results suggest that PS1 and PS2 perform a redundant function in ER Ca^{2+} signaling and that at least one of them is required for pridopidine to lower ER Ca^{2+} levels.

3.6. S1R is required for pridopidine to enhance spine nSOC in PS1-KI hippocampal neurons

Chronically elevated ER calcium levels suppress neuronal store-operated calcium entry (nSOC), leading to destabilization of hippocampal mushroom spines (Sun et al., 2014). Enhancing nSOC either pharmacologically or by overexpression of STIM2 or EB3 prevents mushroom spine loss in hippocampal neurons from PS1-KI mice (Pchitskaya et al., 2017; Sun et al., 2014; Zhang et al., 2016). Consistent with pridopidine's effect on ER calcium levels, we found that it increased nSOC in the spines of cultured PS1-KI neurons expressing GCaMP5G relative to vehicle-treated PS1-KI neurons (Fig. 6A, B). Knockdown of S1R had little effect on spine nSOC in PS1-KI neurons, but prevented the ability of pridopidine to enhance spine nSOC (Fig. 6A, B). Human S1R (hS1R) was overexpression alone had no effect on spine nSOC, but it re-enabled pridopidine to enhance spine nSOC (Fig. 6A, B).

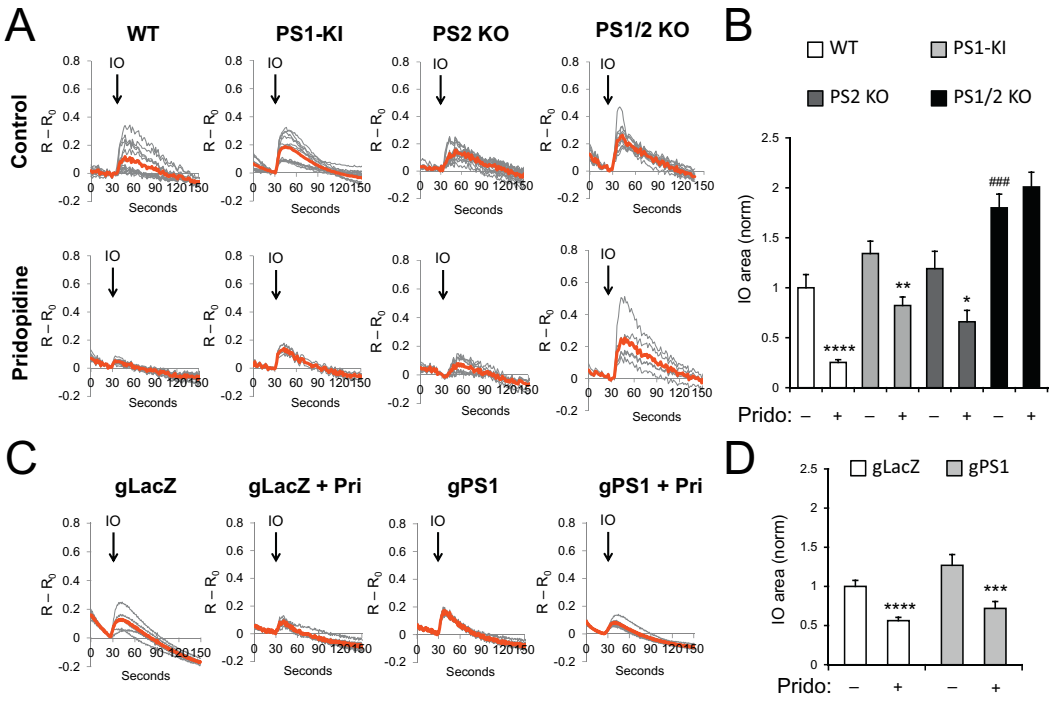

Fig. 5. Pridopidine lowers ER calcium levels in hippocampal neurons, but not in PS1/2 KO hippocampal neurons. (A) Fura-2340/380 fluorescence ratio traces are shown for WT, PS1-KI, PS2 KO (PS2 KO/PS1$^{Flox/Flox}$ infected with lenti-NLS-GFP on DIV7) and PS1/2 KO (PS2 KO/PS1$^{Flox/Flox}$ infected with lenti-NLS-GFP-Cre on DIV7) hippocampal neurons. Regions of interest were placed on cell bodies (red = averaged trace, gray = individual traces). 30 s after removing external calcium, 5 μM ionomycin (IO) was added to release calcium from the ER. Calcium imaging was performed on DIV14–16. Cultures were treated with 1 μM pridopidine for 16–24 h prior to starting the experiment (bottom for each genotype) and the vehicle control (top for each genotype). (B) The size of the IO-sensitive calcium pool was estimated by integrating the area under Fura-2 traces. The results were normalized to the IO-sensitive calcium pool size in WT control cultures. $n = 112$ neurons for WT (10 coverslips), 118 neurons for WT + pridopidine (8 coverslips), 129 neurons for PS1-KI (9 coverslips), 98 neurons for PS1-KI + pridopidine (7 coverslips), 182 neurons for PS2 KO (12 coverslips), 152 neurons for PS2 KO + pridopidine (13 coverslips), 330 neurons for PS1/2 KO (20 coverslips) and 291 neurons for PS1/2 KO + pridopidine (19 coverslips). (C) Fura-2340/380 fluorescence ratio traces are shown for hippocampal cultures infected with lenti-Cas9 and lenti-gLacZ or lenti-gPS1 on DIV7. Calcium imaging was performed on DIV14–16. Cultures were treated with the vehicle or 1 μM pridopidine for 16–24 h prior to starting the experiment. (D) Quantitative summary of the size of the IO-sensitive calcium pool in gLacZ and gPS1 cultures with or without pridopidine treatment. $n = 182$ neurons for gLacZ, 149 neurons for gLacZ + pri, 76 neurons for gPS1 and 118 neurons for gPS1 + Pri. Data was from 9 to 11 coverslips per condition. Mean ± S.E. Pairwise statistical comparisons were made using the Holm-Bonferroni test. *$p < 0.05$. **$p < 0.01$. ***$p < 0.001$. ****$p < 0.0001$. Vehicle-treated experimental conditions were also compared to the vehicle-treated WT control condition. *###p* < .001. (For interpretation of the references to colour in this figure legend, the reader is referred to the web version of this article.)

We then tested whether pridopidine could stabilize mushroom spines of WT and PS1-KI neurons when nSOC is suppressed. We previously discovered that inhibition of nSOC destabilizes hippocampal mushroom spines (Sun et al., 2014). We here confirmed that in WT cultures a 16-h incubation with 10 μM SKF96365 (blocker of TRPC channels) deceased the abundance of mushroom spines (Fig. 7A, B). WT mushroom spines remained sparse even with pridopidine was co-administered with SKF96365 (Fig. 7A, B). As before (Fig. 1F, G), application of 100 nM or 1 μM pridopidine, increased the prevalence of PS1-KI mushroom spines compared to vehicle-treated PS1-KI mushroom spines (Fig. 7C, D). 10 μM SKF96365 did not further decrease the abundance of PS1-KI mushroom spines, but it prevented protection of mushroom spines by pridopidine (Fig. 7C, D). We also repeated this experiment using a CRISPR/Cas9 approach to impede expression of STIM1 (gSTIM1), STIM2 (gSTIM2) or STIM1/2 (gSTIM1/2). Lenti-Cas9/gSTIM1 expression did not affect the prevalence of WT mushroom spines, whereas deletion of either STIM2 or STIM1/2 destabilized WT mushroom spines (Fig. 7E, F). 1 μM pridopidine (16 h starting on DIV15 – DIV16) was unable to stabilize WT spines in the absence of neuronal STIM2 or STIM1/2 spines (Fig. 7E, F). Pridopidine treatment increased the fraction of PS1-KI mushroom spines compared to vehicle-treated PS1-KI mushroom spines (Fig. 7G, H). Deletion of STIM1, STIM2 or STIM1/2 by expression of Cas9 plus gSTIM1 and/or gSTIM2 caused no additional loss of PS1-KI mushroom spines; however, deletion of STIM1, STIM2 or STIM1/2 prevented the rescue of PS1-KI mushroom spines by pridopidine (Fig. 7G, H). Thus, inhibition of nSOC either pharmacologically or by CRISPR/Cas9-mediated deletion of STIM1 and/or STIM2 thwarted the synaptoprotective action of pridopidine. This is consistent with the possibility that pridopidine rescues PS1-KI mushroom spines through upregulation of nSOC pathway activity.

3.7. Oral pridopidine treatment rescues mushroom spines in PS1-KI mice

Finally, we tested whether pridopidine can prevent hippocampal mushroom spine loss *in vivo* in PS1-KI mice. At 5 months of age WT-GFP and PS1-KI-GFP mice began one month of daily treatment with orally administered pridopidine (30 mg / kg) or the vehicle control. At 6 months of aged, mice were exsanguinated and perfused with fixative. Brains were removed, postfixed and then sliced with a vibratome. GFP-positive pyramidal neurons of CA1 were imaged with a confocal, focusing on 2nd-order apical dendrites in the stratum radiatum (Fig. 8A). 8–10 mice were included per condition and 40–50 neurons were imaged per condition. Although there were no significant changes in spine density (for all spine types) from the PS1-KI mutation or pridopidine treatment, we observed a significant decrease in the prevalence of mushroom spines in PS1-KI mice as well as an increase of thin spines in PS1-KI mice (Fig. 8A, B). This suggested a deficit in mushroom spine maturation and/or maintenance in PS1-KI mice, consistent with our previous findings (Sun et al., 2014; Zhang et al., 2016). Treatment with pridopidine normalized the prevalence of both mushroom and thin

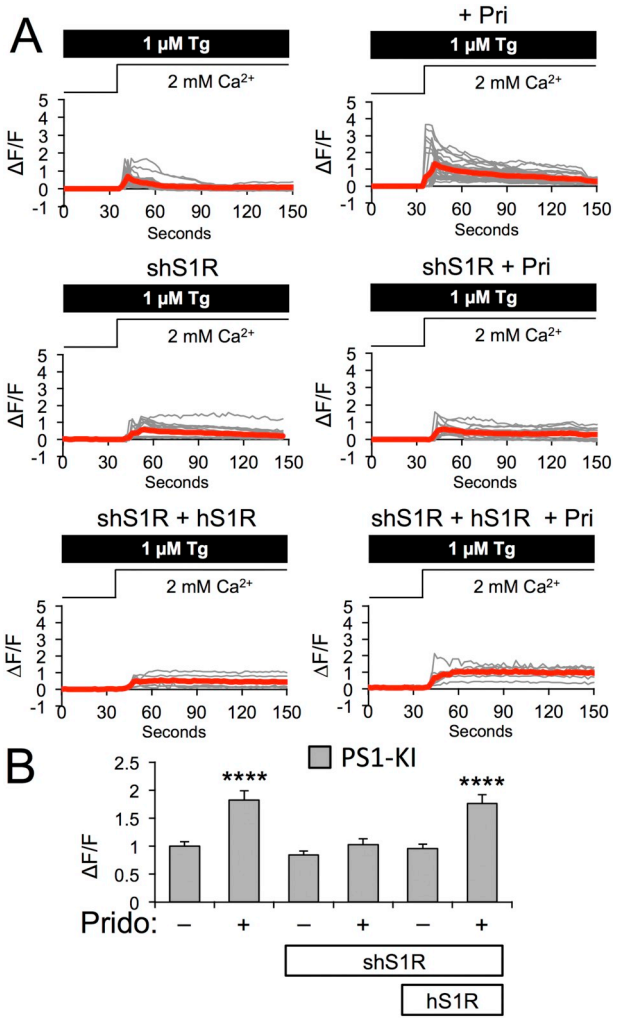

Fig. 6. S1R is required for pridopidine to enhance spine nSOC in PS1-KI hippocampal neurons. (A) GCaMP5G fluorescence traces from spines of PS1-KI hippocampal neurons during the calcium "add-back" protocol for nSOC measurement (red = averaged trace, gray = individual traces). To deplete ER calcium, external calcium was calcium removed and 1 μM thapsigargin (Tg) was added to block SERCA pump activity 10 min prior to adding 2 mM calcium back to the ACSF. Cultures were infected with lenti-scrambled shRNA (top), lenti-shRNA targeting mouse S1R (shS1R; bottom), or lenti-shS1R and lenti-human S1R (hS1R) to restore S1R expression on DIV7 and treated with the vehicle (left) or 1 μM pridopidine (right) for 16–24 h starting on DIV14. (B) The peak of spine nSOC was quantified. Results were normalized to PS1-KI control cultures and are shown as mean ± S.E. $n = 84$ spines for control shRNA (10 coverslips), 63 spines for control shRNA + pridopidine (7 coverslips), 94 spines for shS1R (10 coverslips), 80 spines for shS1R + pridopidine (9 coverslips), 100 spines for shS1R + hS1R (10 coverslips) and 65 spines for shS1R + hS1R + pridopidine (7 coverslips). Comparisons to the PS1-KI control condition were made with the Holm-Bonferroni test. ****$p < 0.0001$. (For interpretation of the references to colour in this figure legend, the reader is referred to the web version of this article.)

spines from PS1-KI mice (Fig. 8A, B), suggesting that it promotes mushroom spine stability *in vivo*.

4. Discussion

4.1. S1R as a target for pridopidine in AD

S1R agonists are procognitive, synaptogenetic and neuroprotective in conditions of neuronal stress (Antonini et al., 2009; Bolshakova et al., 2016; Hindmarch and Hashimoto, 2010; Ruscher et al., 2011) and as a result they are beneficial in experimental models of Huntington's disease (HD) (Bol'shakova et al., 2017; Ryskamp et al., 2017; Squitieri et al., 2015; Garcia-Miralles et al., 2017; Geva et al., 2016; Kusko et al., 2018), Parkinson's disease (Francardo et al., 2014) and AD (Fisher et al., 2016; Hall et al., 2017; Maurice and Goguadze, 2017; Meunier et al., 2006). For example, we discovered that the mixed muscarinic/S1R agonist AF710B prevents the loss of mushroom spines in hippocampal cultures prepared from APP-KI or PS1-KI mice (Fisher et al., 2016). We also found that pridopidine and 3-PPP were synaptoprotective in a mouse model of HD (Ryskamp et al., 2017). We further demonstrated that pridopidine activates neuroprotective pathways impaired in HD and improves behavioural and transcriptional deficits in HD mice (Garcia-Miralles et al., 2017; Geva et al., 2016; Kusko et al., 2018).

Several lines of evidence point to the potential involvement of S1R in AD. The S1R polymorphisms Q2P and C240T/G241 T may influence risk of developing AD in carriers of the APOE ε4 allele (Fehér et al., 2012; Huang et al., 2011; Maruszak et al., 2007; Uchida et al., 2005). The C240T/G241 T allele decreases expression of S1R (Mishina et al., 2008), which is significant because downregulation of S1R may contribute to AD pathology. The density of S1R binding sites was reduced in several brain regions early in AD in PET imaging experiments with S1R radioligands (Mishina et al., 2008). Decreased S1R radioligand binding was also observed in cadavers in the CA1 area of the anterior hippocampus (Jansen et al., 1993). This was correlated to pyramidal cell loss (Jansen et al., 1993), consistent with a role for S1R in supporting the long-term viability of hippocampal neurons. Our results (Fig. 3) and previously published studies (Fisher et al., 2016; Tsai et al., 2009) demonstrated that knockdown of S1R in hippocampal neurons leads to a loss of synaptic spines. Thus, S1R downregulation could contribute to the neuropathology of AD. Another reason why S1R downregulation in AD patients might worsen pathology is that S1R protects against tau hyperphosphorylation by promoting degradation of p35, an activator cyclin-dependent kinase 5 (cdk5) (Tsai et al., 2015).

Based on these findings we tested whether pridopidine and 3-PPP are synaptoprotective in models of AD and whether this requires S1R. We found that pridopidine and the chemically similar S1R agonist 3-PPP rescued mushroom spine loss in multiple mouse models of AD (Aβ oligomer toxicity, APP-KI, PS1-KI) (Fig. 1). Interestingly, pre-incubation with low (nanomolar) pridopidine concentrations reversed hippocampal LTP defects induced by application of $A\beta_{42}$ oligomers (Fig. 2).

Either pharmacological inhibition or knockdown of S1R prevented the rescue of mushroom spines by pridopidine (Fig. 3), demonstrating that S1R is a primary target of pridopidine. This is consistent with the high affinity of pridopidine for S1R (Sahlholm et al., 2013; Sahlholm et al., 2015). These results indicate that the beneficial actions of pridopidine are likely to be mediated via activation of S1R, resulting in bolstering of AD mushroom spines. We also found that oral pridopidine treatment could stabilize mushroom spines *in vivo* in aged PS1-KI mice (Fig. 8), suggesting that pridopidine might act as a disease-modifying therapeutic in AD.

4.2. Effects of pridopidine on LTP and mushroom spines

As LTP causes mushroom spine formation (Bourne and Harris, 2007) and blockade of LTP by $A\beta_{42}$ application leads to a reduction in spine abundance (Rammes et al., 2018), the reversal of LTP deficits and mushroom spine loss by pridopidine may involve the same mechanism. Indeed, both LTP and mushroom spine formation are largely induced by NMDA receptor currents (Matsuzaki et al., 2004; Noguchi et al., 2005) and S1R activity is thought to promote NMDA receptor function (Martina et al., 2007; Waters et al., 2018), possibly through increased trafficking to the plasma membrane (Pabba et al., 2014). Thus, facilitation of NMDA receptor activity may have contributed to the rescue of LTP and mushroom spine loss caused by $A\beta_{42}$ oligomer toxicity. Pre-incubation of CA1 pyramidal neurons with 30 nM pridopidine had no

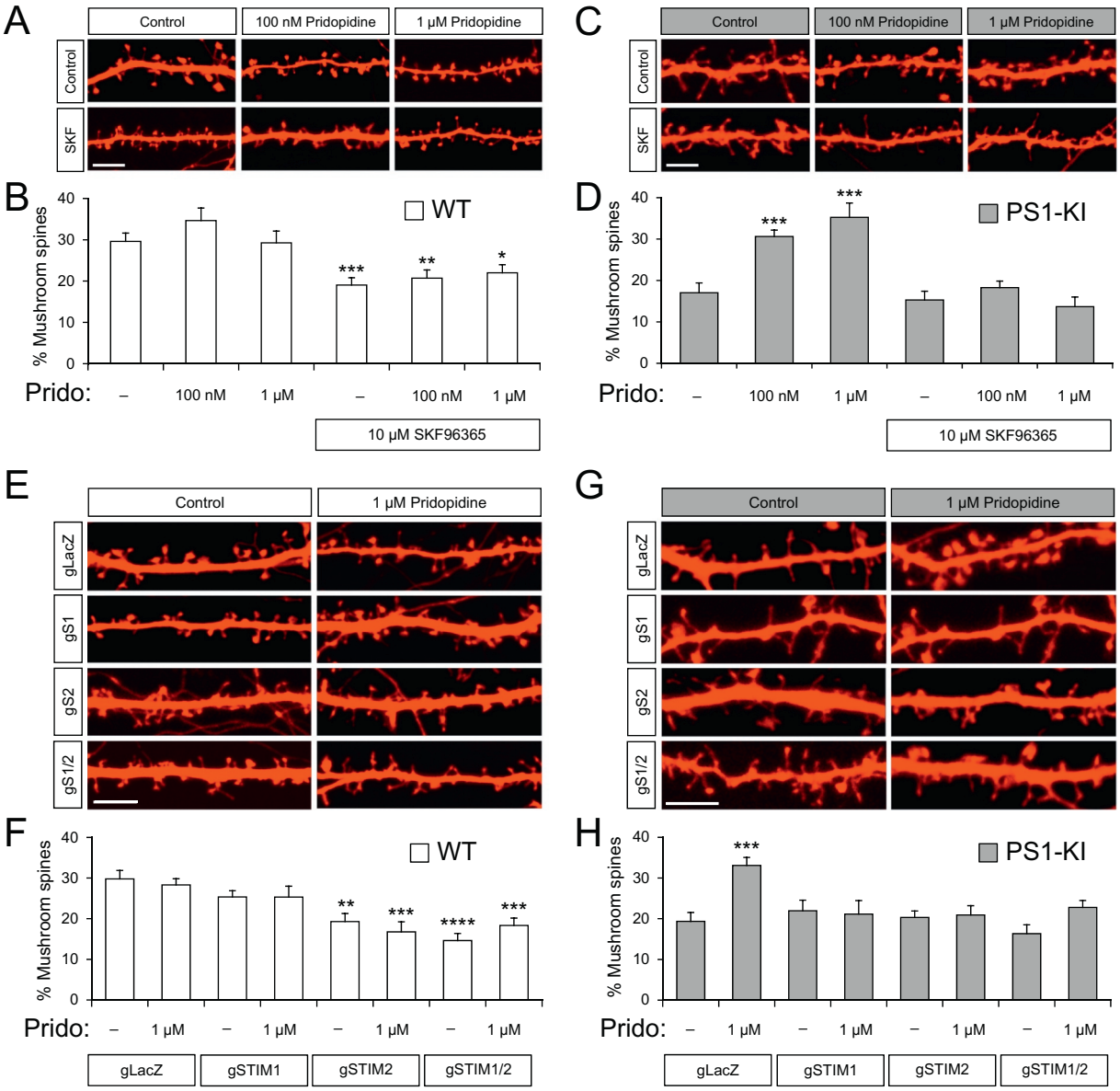

Fig. 7. Pridopidine is unable to rescue PS1-KI mushroom spines during nSOC inhibition. (A) Confocal images of spines expressing TdTomato in WT hippocampal cultures. Scale bar = 5 μm. (B) Quantitative summary of mushrooms spine prevalence in WT hippocampal cultures treated for 16 h on DIV15–16 with the vehicle, 100 nM pridopidine, 1 μM pridopidine and/or 10 μM SKF96365. *n* = 15 neurons per condition. (C) Confocal images of spines expressing TdTomato in PS1-KI hippocampal cultures. Scale bar = 5 μm. (D) Quantitative summary of mushrooms spine prevalence in PS1-KI hippocampal cultures treated for 16 h on DIV15–16 with the vehicle, 100 nM pridopidine, 1 μM pridopidine and/or 10 μM SKF96365. n = 9 neurons for the vehicle control, 6 neurons for 100 nM pridopidine, 11 neurons for 1 μM pridopidine, 13 neurons for SKF96365, 6 neurons for SKF96365 + 100 nM pridopidine and 12 neurons for SKF96365 + 1 μM pridopidine. (E) Confocal images of spines expressing TdTomato in WT hippocampal cultures infected on DIV7 with lenti-Cas9 and lenti-gLacZ (gLacZ), lenti-gSTIM1 (gSTIM1), lenti-gSTIM2 (gSTIM2), or lenti-gSTIM1/2 (gSTIM1). Scale bar = 5 μm. (F) Quantitative summary of mushrooms spine prevalence in lenti-virus infected WT hippocampal cultures treated for 16 h on DIV15–16 with the vehicle or 1 μM pridopidine. n = 11–12 neurons per condition. (G) Confocal images of spines expressing TdTomato in PS1-KI hippocampal cultures infected on DIV7 with lenti-Cas9 and lenti-gLacZ (gLacZ), lenti-gSTIM1 (gSTIM1), lenti-gSTIM2 (gSTIM2), or lenti-gSTIM1/2 (gSTIM1). Scale bar = 5 μm. (H) Quantitative summary of mushrooms spine prevalence in lenti-virus infected PS1-KI hippocampal cultures treated for 16 h on DIV15–16 with the vehicle or 1 μM pridopidine. *n* = 10 neurons for PS1-KI and PS1-KI + pridopidine, 11 neurons for gSTIM1, 15 neurons for gSTIM1 + pridopidine, 19 neurons for gSTIM2, 15 neurons for gSTIM2 + pridopidine, 13 neurons for gSTIM1/2 and 16 neurons for gSTIM1/2 + pridopidine. Experimental conditions were compared to the control condition using the Holm-Bonferroni test. *p < 0.05. **p < 0.01. ***p < 0.001. ****p < 0.0001.

effect on basal LTP (Fig. 2A and B), but LTP was slightly reduced by 100 nM pridopidine (Fig. 2C and D). The reason for the effect of 100 nM pridopidine is not completely clear. Both concentrations of pridopidine mitigated the LTP deficit from $A\beta_{42}$, which is consistent with the prevention of mushroom spine loss from $A\beta_{42}$ oligomers. Although 100 nM pridopidine slightly reduced synaptic strength *per se*, we did not detect a reduction in mushroom spine prevalence following treatment with pridopidine. The reason for the discrepancy is unclear, but it suggests that the effect of pridopidine on LTP and mushroom spines prevalence may be time-dependent, because hippocampal slices were treated with pridopidine for 60 min prior to LTP induction, whereas hippocampal cultures were treated with pridopidine for 16 h prior to fixation for analysis of spine morphology.

S1R knockout mice have a slight, but significant deficit in LTP (Snyder et al., 2016) and a mild impairment in spatial memory is observed in female S1R KO mice (Chevallier et al., 2011). The phenotype of S1R KO mice is milder than expected given mushroom spine loss in the abence of S1R in cultures. However, constitutive knockouts often

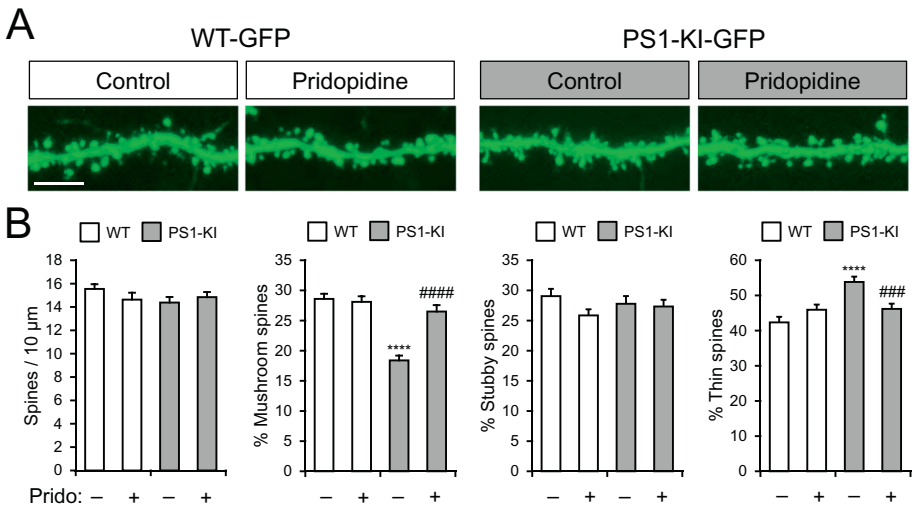

Fig. 8. Oral pridopidine treatment rescues mushroom spines in PS1-KI mice. (A) Confocal images of CA1 pyramidal neuron apical spines in brain slices from WT-GFP and PS1-KI-GFP mice aged to 6 months. Scale bar = 5 µm. (B) Quantitative summary of dendritic spine density (all spine types) and the prevalence of mushroom spines, stubby spines and thin spines in hippocampal neurons from WT-GFP and PS1-KI-GFP mice. Pridopidine (30 mg/kg) or the vehicle was administered daily over 1 month starting when mice were at 5 months of age. $n = 45$ neurons for WT-GFP control (9 mice), $n = 50$ neurons for WT-GFP + pridopidine (10 mice), $n = 40$ neurons for PS1-KI-GFP (8 mice) and n = 40 neurons for PS1-KI-GFP + pridopidine (8 mice). Experimental conditions were compared to the WT control condition (****$p < 0.0001$) and the pridopidine-treated PS1-KI condition was compared to the vehicle-treated PS1-KI control condition (###$p < 0.001$ and ####$p < 0.0001$) using the Holm-Bonferroni test. Scale bar = 5 µm.

have compensatory effects, whereas knockdowns could produce a more substantial phenotype before compensation occurs.

4.3. Effects on calcium signaling from S1R activation by pridopidine

Given S1R's well-established modulatory role on ER calcium signaling (Hayashi and Su, 2007; Srivats et al., 2016), we evaluated whether pridopidine stabilizes calcium homeostasis in cultured hippocampal neurons from WT, PS1-KI and conditional presenilin double-knockout mice ($PS1^{flox/flox}$, $PS2^{-/-}$) infected with lenti-NLS-GFP or lenti-NLS-Cre viruses as well as in neurons expressing Cas9/gPS1. A 16–24 h treatment with pridopidine lowered ER calcium levels in WT, gPS1, PS1-KI and PS2 KO neurons, but not PS1/2 KO neurons (Fig. 5) and pridopidine treatment rescued mushroom spines in PS1-KI, gPS1 and PS2 KO neurons, but not PS1/2 KO neurons (Fig. 4). The lack of an effect in PS1/2 KO neurons implies that a functional ER calcium leak pathway (Nelson et al., 2007; Tu et al., 2006a) is required for pridopidine to lower ER calcium levels and stabilize mushroom spines. The reason for this requirement is unclear, but it could entail S1R enhancing calcium leakage from the ER either by modulating leak activity of PS channels or regulating the abundance of PS holoprotein in the ER membrane. It is enticing to speculate that S1R could somehow interfere with catalytic cleavage of PS1 and thereby limit its incorporation/function in the γ-secretase complex. This might explain how S1R agonists decrease the burden of amyloid plaques (Fisher et al., 2016). Future studies are needed to clarify how pridopidine regulates ER calcium levels in hippocampal neurons and how S1R agonists reduce $A\beta_{42}$ accumulation and aggregation. Consistent with this spine loss phenotype from PS1 and/or PS2 KO, mild cognitive deficits result from condition inactivation of PS1 in the mouse forebrain, whereas inactivation of both PS1 and PS2 results in severe deficits in cognitive performance and synaptic plasticity, eventually leading to overt neurodegeneration (Sun et al., 2005).

The reduction of ER calcium levels by pridopidine is expected to increase nSOC, upregulation of which stabilizes mushroom spines (Sun et al., 2014). As nSOC is impaired in PS1-KI spines compared to WT spines (Sun et al., 2014), we tested whether pridopidine might stabilize PS1-KI mushroom spines by enhancing spine nSOC. A 16–24 h treatment with pridopidine elevated nSOC in PS1-KI spines and this required S1R (Fig. 6). Thus, pridopidine may reinstate mushroom spine stability in PS1-KI neurons through augmenting signaling in the spine nSOC pathway. This was supported by data showing that inhibition or genetic ablation of nSOC activity prevents pridopidine from stabilizing PS1-KI mushroom spines (Fig. 7).

In contrast, S1R overexpression or incubation with S1R agonists suppresses SOC in other cell types (Brailoiu et al., 2016; Srivats et al., 2016), possibly from S1R binding to STIM1 and obstructing the interaction of STIM1 and Orai1 (Srivats et al., 2016). Also, pridopidine suppresses supranormal nSOC below synaptotoxic levels in cultured medium spiny neurons from YAC128 mice that model Huntington's disease (Ryskamp et al., 2017). nSOC is excessive in this context because mutant Huntingtin protein sensitizes $InsP_3R1$ to $InsP_3$, causing leakage of calcium from the ER and activation of nSOC (Tang et al., 2003; Wu et al., 2018; Wu et al., 2016; Wu et al., 2011). Pridopidine normalizes calcium homeostasis in YAC128 medium spiny neurons by negatively modulating $InsP_3R1$ (Ryskamp et al., 2017). However, in the present experiments pridopidine decreased ER calcium levels and enhanced nSOC. This discrepancy suggests that the action of S1R in a given cell type reflects the assortment of client proteins that S1R can modulate. For example, although $InsP_3R1$ represents a primary ER calcium release pathway in medium spiny neurons (Wu et al., 2016), presenilins represent a primary pathway for ER calcium leakage in hippocampal neurons (Nelson et al., 2007; Tu et al., 2006a; Zhang et al., 2010). Also, although S1R can suppress STIM1-dependent SOC, STIM2 is the primary activator of nSOC in hippocampal neurons (Sun et al., 2014). Perhaps, S1R does not bind and sequester STIM2 or if S1R does bind STIM2, it might either have a neutral or a positive modulatory effect on STIM2-gated nSOC. Either way, decreased ER calcium levels in hippocampal neurons from pridopidine treatment would increase the activation of nSOC and this could explain the results. In addition, activation of S1R by pridopidine might lead to actin remodeling in spines and/or reduced oxidative stress (Tsai et al., 2009). Taken together, our data suggests that the ability of pridopidine to stabilize hippocampal mushroom spines in neurons from AD models may involve modulation of ER Ca^{2+} signaling and the nSOC pathway.

4.4. Roles of S1R in regulating neurophysiology and mushroom spine dynamics

The S1R modulates neurophysiology through a number of pathways including voltage-gated ion channels (Kourrich et al., 2012), $InsP_3Rs$ (Hayashi and Su, 2007; Ryskamp et al., 2017) and nSOC channels (Ryskamp et al., 2017). S1R also modulates hippocampal neuron firing from NMDA receptor activation (Martina et al., 2007; Monnet et al., 1990; Pabba et al., 2014) and other aspects of neuronal functioning via cAMP, cFos, Bcl-2, NFκB, and CREB (Meunier and Hayashi, 2010). NMDA receptors play a major role in hippocampal LTP (Lu et al., 2001), spine maturation (Tada and Sheng, 2006), and learning (Morris et al., 1986). S1R positively regulates NMDA receptor function in hippocampal neurons (Monnet et al., 1990; Monnet et al., 1995), possibly by

modulating the response to NMDA-mediated calcium signals (e.g., by suppressing potassium efflux via SK channels) and increasing expression and trafficking of NMDA receptors to the plasma membrane (Martina et al., 2007; Pabba et al., 2014). This could facilitate maturation of mushroom spines in response to stimulation with S1R agonists. Thus, through pleiotropic actions S1R regulates a multitude of proteins, fine-tuning the activity of ion channels in the ER and plasma membrane as well as many other biochemical processes. This culminates in diverse roles for S1R in neuromodulation, synaptic plasticity, learning and memory, and neuroprotection.

Prior studies indicated that S1R regulates dendritic spine size in hippocampal neurons, as well as oxidative stress and Rac-GTP signaling (Tsai et al., 2009). A microarray study found that S1R knockdown in cultured hippocampal neurons affects transcription in several pathways including those involved in sterol biosynthesis, protein ubiquitination, the actin cytoskeleton network and oxidative stress (Tsai et al., 2012). S1R-dependent regulation of oxidative stress could be important for hippocampal synapses as spine deficits from S1R knockdown were rescued by reducing oxidative stress (Tsai et al., 2009). Consistent with these studies, we found that pharmacological inhibition or knockdown of S1R led to loss of mushroom spines in WT hippocampal cultures (Fig. 3B, C), confirming an essential role of S1R in the development and/or maintenance of robust synaptic connections within the hippocampus. Interestingly, memory impairment is a common side effect of the anti-psychotic drug and S1R antagonist haloperidol (K_D for S1R ~3 nM) (Abdel-Salam et al., 2012), which could be related to destabilization of hippocampal mushroom spines. The loss of mushroom spines in WT hippocampal neurons from S1R inhibition suggests that although S1R behaves as a ligand-operated chaperone, it possesses basal activity that is important for spine stability. However, the basal activity of S1R is unable to prevent spine loss from AD-related stress, even when S1R is overexpressed (Fig. 3B, C). It is unclear whether endogenous ligands control basal S1R activity and if their signaling changes to compensate for cellular stress in AD. S1R activity may be regulated by endogenous ligands such as steroid hormones (e.g., DHEA sulfate, pregnenolone sulfate and progesterone), membrane lipids (D-erythro-shingosine, sphinganine and ceramides), neuropeptides (e.g., neuropeptide Y), and the trace amine *N,N*-dimethyltryptamine (Fontanilla et al., 2009; Maurice and Su, 2009; Meurs et al., 2007; Su et al., 2010). S1R activity may also be modulated by physiological changes including changes in ER calcium content, ER stress (Hayashi and Su, 2007) and oxidative stress (Meunier and Hayashi, 2010). Our data suggests that under conditions of chronic neuronal stress, S1R activity may benefit from a pharmacological boost to counteract the neurochemical changes in neurodegenerative diseases.

5. Conclusions

Mushroom spines are destabilized by calcium dysregulation in multiple mouse models of AD. Pridopidine facilitates calcium signals that support mushroom spines formation and/or maintenance in cultured APP-KI neurons, PS1-KI neurons and neurons exposed to synaptotoxic $A\beta_{42}$ oligomers. The actions of pridopidine in hippocampal neurons are mediated by S1R, which is necessary for mushroom spine stability in WT hippocampal neurons. By decreasing ER calcium levels (possibly through promoting ER calcium leakage), pridopidine enhances nSOC activity, thereby stabilizing mushroom spines *in vitro* and *in vivo*. In addition, pre-incubation of CA1 pyramidal neurons with low pridopidine concentrations counteracts the synaptotoxic effects of $A\beta_{42}$ oligomers on LTP. These data suggest that pridopidine might act as a disease-modifying and neuroprotective therapeutic in AD by stimulating S1R activity. The presented data also provide insights into pridopidine's mechanism of action and highlight the S1R as a potential target for treating AD.

Competing interests

TEVA Pharmaceuticals provided funding for the portions of the study. M.G. and M.H are employees of TEVA Pharmaceuticals and I.B. is a paid consultant to TEVA Pharmaceuticals. MG., I.B. and H.M. filed a patent application pertaining to this research: Geva, M., Bezprozvanny, I., Bassan, M., & Hayden, M. (2016). U.S. Patent Application No. 15/052,368. The remaining authors declare no competing financial interests. No non-financial conflicts of interest exist for any of the authors.

Authors' contributions

DR performed most experiments and analysis, interpreted the data, participated in design of the study and drafted the manuscript; DR, LW performed *in vitro* mushroom spine loss assay experiments and analysis; DK, GR performed LTP experiments and analysis; DR, JW performed calcium-imaging experiments on SH-SY5Y cells; MG provided critical feedback and suggestions; DR, MH, IB conceived the study and participated in its design and coordination; DR, MG, MH, GR, IB helped to revise the manuscript. All authors read and approved the final manuscript.

Acknowledgements

We are grateful to members of the Ilya Bezprozvanny laboratory for advice and suggestions, Leah Taylor and Pippa Loupe for administrative assistance, and Qianmei Yang for technical assistance with brain slicing. We also thank Pippa Loupe and Juha Savola for editorial suggestions. The research described herein was supported by TEVA Pharmaceuticals, Israel (SRA #109415, IB), by the grants from the National Institutes of Health (R01NS080152 and R01AG055577, IB; F32NS093786, DAR) and by the Russian Science Foundation Grant (14-25-00024-П, IB). IB holds the Carl J. and Hortense M. Thomsen Chair in Alzheimer's Disease Research.

References

Abdel-Salam, O.M., El-Shamarka, M.E.-S., Salem, N.A., El-Mosallamy, A.E., Sleem, A.A., 2012. Amelioration of the haloperidol-induced memory impairment and brain oxidative stress by cinnarizine. EXCLI J. 11, 517.

Alzheimer's, A., 2015. Alzheimer's disease facts and figures. Alzheimer's Dementia 11, 332.

Anderson, W.W., Collingridge, G.L., 2001. The LTP Program: a data acquisition program for on-line analysis of long-term potentiation and other synaptic events. J. Neurosci. Methods 108, 71–83.

Antonini, V., Prezzavento, O., Coradazzi, M., Marrazzo, A., Ronsisvalle, S., Arena, E., Leanza, G., 2009. Anti-amnesic properties of (±)-PPCC, a novel sigma receptor ligand, on cognitive dysfunction induced by selective cholinergic lesion in rats. J. Neurochem. 109, 744–754.

Bolshakova, A.V., Kukanova, E.O., Gainullina, A.N., Zhemkov, V.A., Korban, S.A., Bezprozvanny, I.B., 2016. Sigma-1 receptor as a potential pharmacological target for the treatment of neuropathology. Phys. Mathem. 2, 31–40.

Bol'shakova, A., Kraskovskaya, N., Gainullina, A., Kukanova, E., Vlasova, O., Bezprozvanny, I., 2017. Neuroprotective effect of σ1-receptors on the cell model of Huntington's disease. Bull. Exp. Biol. Med 1–7.

Bourne, J., Harris, K.M., 2007. Do thin spines learn to be mushroom spines that remember? Curr. Opin. Neurobiol. 17, 381–386.

Brailoiu, G.C., Deliu, E., Console-Bram, L.M., Soboloff, J., Abood, M.E., Unterwald, E.M., Brailoiu, E., 2016. Cocaine inhibits store-operated Ca2+ entry in brain microvascular endothelial cells: critical role for sigma-1 receptors. Biochem. J. 473, 1–5.

Bromer, C., Bartol, T.M., Bowden, J.B., Hubbard, D.D., Hanka, D.C., Gonzalez, P.V., Kuwajima, M., Mendenhall, J.M., Parker, P.H., Abraham, W.C., 2018. Long-term potentiation expands information content of hippocampal dentate gyrus synapses. Proc. Natl. Acad. Sci. 115, E2410–E2418.

Brookmeyer, R., Abdalla, N., Kawas, C.H., Corrada, M.M., 2018. Forecasting the prevalence of preclinical and clinical Alzheimer's disease in the United States. Alzheimers Dement. 14, 121–129.

Brune, S., Schepmann, D., Klempnauer, K.H., Marson, D., Dal Col, V., Laurini, E., Fermeglia, M., Wunsch, B., Pricl, S., 2014. The sigma enigma: in vitro/in silico site-directed mutagenesis studies unveil sigma1 receptor ligand binding. Biochemistry 53, 2993–3003.

Chevallier, N., Keller, E., Maurice, T., 2011. Behavioural phenotyping of knockout mice for the sigma-1 (σ1) chaperone protein revealed gender-related anxiety, depressive-like and memory alterations. J. Psychopharmacol. 25, 960–975.

De Felice, F.G., Velasco, P.T., Lambert, M.P., Viola, K., Fernandez, S.J., Ferreira, S.T., Klein, W.L., 2007. Abeta oligomers induce neuronal oxidative stress through an N-methyl-D-aspartate receptor-dependent mechanism that is blocked by the Alzheimer drug memantine. J. Biol. Chem. 282, 11590–11601.
de Yebenes, J.G., Landwehrmeyer, B., Squitieri, F., Reilmann, R., Rosser, A., Barker, R.A., Saft, C., Magnet, M.K., Sword, A., Rembratt, A., Tedroff, J., Mermai, H.D., 2011. Pridopidine for the treatment of motor function in patients with Huntington's disease (MermaiHD): a phase 3, randomised, double-blind, placebo-controlled trial. Lancet Neurol. 10, 1049–1057.
Dyhring, T., Nielsen, E.O., Sonesson, C., Pettersson, F., Karlsson, J., Svensson, P., Christophersen, P., Waters, N., 2010. The dopaminergic stabilizers pridopidine (ACR16) and (−)-OSU6162 display dopamine D(2) receptor antagonism and fast receptor dissociation properties. Eur. J. Pharmacol. 628, 19–26.
Esmaeilzadeh, M., Kullingsjö, J., Ullman, H., Varrone, A., Tedroff, J., 2011. Regional cerebral glucose metabolism after pridopidine (ACR16) treatment in patients with Huntington disease. Clin. Neuropharmacol. 34, 95–100.
Fehér, Á., Juhász, A., László, A., Kálmán, J., Pákáski, M., Janka, Z., 2012. Association between a variant of the sigma-1 receptor gene and Alzheimer's disease. Neurosci. Lett. 517, 136–139.
Feng, G., Mellor, R.H., Bernstein, M., Keller-Peck, C., Nguyen, Q.T., Wallace, M., Nerbonne, J.M., Lichtman, J.W., Sanes, J.R., 2000. Imaging neuronal subsets in transgenic mice expressing multiple spectral variants of GFP. Neuron 28, 41–51.
Fisher, A., Bezprozvanny, I., Wu, L., Ryskamp, D.A., Bar-Ner, N., Natan, N., Brandeis, R., Elkon, H., Nahum, V., Gershonov, E., LaFerla, F.M., Medeiros, R., 2016. AF710B, a novel M1/σ1 agonist with therapeutic efficacy in animal models of Alzheimer's disease. Neurodegenerative Dis. 16, 95–110.
Fontanilla, D., Johannessen, M., Hajipour, A.R., Cozzi, N.V., Jackson, M.B., Ruoho, A.E., 2009. The hallucinogen N, N-dimethyltryptamine (DMT) is an endogenous sigma-1 receptor regulator. Science 323, 934–937.
Francardo, V., Bez, F., Wieloch, T., Nissbrandt, H., Ruscher, K., Cenci, M.A., 2014. Pharmacological stimulation of sigma-1 receptors has neurorestorative effects in experimental parkinsonism. Brain 137, 1998–2014.
Garcia-Miralles, M., Geva, M., Tan, J.Y., Yusof, N., Cha, Y., Kusko, R., Tan, L.J., Xu, X., Grossman, I., Orbach, A., Hayden, M.R., Pouladi, M.A., 2017. Early Pridopidine Treatment Improves Behavioral and Transcriptional Deficits in YAC128 Huntington Disease Mice. (JCI Insight. 2).
Geva, M., Kusko, R., Soares, H., Fowler, K.D., Birnberg, T., Barash, S., Wagner, A.M., Fine, T., Lysaght, A., Weiner, B., Cha, Y., Kolitz, S., Towfic, F., Orbach, A., Laufer, R., Zeskind, B., Grossman, I., Hayden, M.R., 2016. Pridopidine activates neuroprotective pathways impaired in Huntington Disease. Hum. Mol. Genet. 25, 3975–3987.
Guo, Q., Fu, W., Sopher, B.L., Miller, M.W., Ware, C.B., Martin, G.M., Mattson, M.P., 1999. Increased vulnerability of hippocampal neurons to excitotoxic necrosis in presenilin-1 mutant knock-in mice. Nat. Med. 5, 101–106.
Hall, H., Iulita, M.F., Gubert, P., Aguilar, L.F., Ducatenzeiler, A., Fisher, A., Cuello, A.C., 2017. AF710B, an M1/sigma-1 receptor agonist with long-lasting disease-modifying properties in a transgenic rat model of Alzheimer's disease. Alzheimer's & Dementia 14, 811–823.
Hayashi, T., Su, T.P., 2007. Sigma-1 receptor chaperones at the ER-mitochondrion interface regulate Ca(2+) signaling and cell survival. Cell 131, 596–610.
Hayashi-Takagi, A., Yagishita, S., Nakamura, M., Shirai, F., Wu, Y.I., Loshbaugh, A.L., Kuhlman, B., Hahn, K.M., Kasai, H., 2015. Labelling and optical erasure of synaptic memory traces in the motor cortex. Nature 525, 333–338.
Hindmarch, I., Hashimoto, K., 2010. Cognition and depression: the effects of fluvoxamine, a sigma-1 receptor agonist, reconsidered. Hum. Psychopharmacol. Clin. Exp. 25, 193–200.
Huang, Y., Zheng, L., Halliday, G., Dobson-Stone, C., Wang, Y., Tang, H.-D., Cao, L., Deng, Y.-L., Wang, G., Zhang, Y.-M., 2011. Genetic polymorphisms in sigma-1 receptor and apolipoprotein E interact to influence the severity of Alzheimer's disease. Curr. Alzheimer Res. 8, 765–770.
Huntington Study Group, 2013. A randomized, double-blind, placebo-controlled trial of pridopidine in Huntington's disease. Mov. Disord. 28, 1407–1415.
Jansen, K., Faull, R., Storey, P., Leslie, R., 1993. Loss of sigma binding sites in the CA1 area of the anterior hippocampus in Alzheimer's disease correlates with CA1 pyramidal cell loss. Brain Res. 623, 299–302.
Jiang, M., Chen, G., 2006. High Ca2+ −phosphate transfection efficiency in low-density neuronal cultures. Nat. Protoc. 1, 695–700.
Kourrich, S., Su, T.P., Fujimoto, M., Bonci, A., 2012. The sigma-1 receptor: roles in neuronal plasticity and disease. Trends Neurosci. 35, 762–771.
Kumar, A., Singh, A., 2015. A review on Alzheimer's disease pathophysiology and its management: an update. Pharmacol. Rep. 67, 195–203.
Kusko, R., Dreymann, J., Ross, J., Cha, Y., Escalante-Chong, R., Garcia-Miralles, M., Tan, L.J., Burczynski, M.E., Zeskind, B., Laifenfeld, D., Pouladi, M., Geva, M., Grossman, I., Hayden, M.R., 2018. Large-scale transcriptomic analysis reveals that pridopidine reverses aberrant gene expression and activates neuroprotective pathways in the YAC128 HD mouse. Mol. Neurodegener. 13, 25.
Lei, M., Xu, H., Li, Z., Wang, Z., O'Malley, T.T., Zhang, D., Walsh, D.M., Xu, P., Selkoe, D.J., Li, S., 2016. Soluble Aβ oligomers impair hippocampal LTP by disrupting glutamatergic/GABAergic balance. Neurobiol. Dis. 85, 111–121.
Lu, W.-Y., Man, H.-Y., Ju, W., Trimble, W.S., MacDonald, J.F., Wang, Y.T., 2001. Activation of synaptic NMDA receptors induces membrane insertion of new AMPA receptors and LTP in cultured hippocampal neurons. Neuron 29, 243–254.
Lublin, A.L., Gandy, S., 2010. Amyloid-β Oligomers: possible Roles as Key Neurotoxins in Alzheimer's Disease. Mount Sinai J. Med. 77, 43–49.
Lundin, A., Dietrichs, E., Haghighi, S., Göller, M.-L., Heiberg, A., Loutfi, G., Widner, H., Wiktorin, K., Wiklund, L., Svenningsson, A., 2010. Efficacy and safety of the dopaminergic stabilizer Pridopidine (ACR16) in patients with Huntington's disease. Clin. Neuropharmacol. 33, 260–264.
Mancuso, R., Oliván, S., Rando, A., Casas, C., Osta, R., Navarro, X., 2012. Sigma-1R agonist improves motor function and motoneuron survival in ALS mice. Neurotherapeutics 9, 814–826.
Martina, M., Turcotte, M.E.B., Halman, S., Bergeron, R., 2007. The sigma-1 receptor modulates NMDA receptor synaptic transmission and plasticity via SK channels in rat hippocampus. J. Physiol. 578, 143–157.
Maruszak, A., Safranow, K., Gacia, M., Gabryelewicz, T., Slowik, A., Styczynska, M., Peplonska, B., Golan, M.P., Zekanowski, C., Barcikowska, M., 2007. Sigma receptor type 1 gene variation in a group of polish patients with Alzheimer's disease and mild cognitive impairment. Dement. Geriatr. Cogn. Disord. 23, 432–438.
Matsuzaki, M., Honkura, N., Ellis-Davies, G.C., Kasai, H., 2004. Structural basis of long-term potentiation in single dendritic spines. Nature 429, 761.
Maurice, T., Goguadze, N., 2017. Sigma-1 (σ1) receptor in memory and neurodegenerative diseases. Sigma Proteins 244, 81.
Maurice, T., Lockhart, B.P., 1997. Neuroprotective and anti-amnesic potentials of sigma (σ) receptor ligands. Prog. Neuro-Psychopharmacol. Biol. Psychiatry 21, 69–102.
Maurice, T., Su, T.-P., 2009. The pharmacology of sigma-1 receptors. Pharmacol. Ther. 124, 195–206.
Maurice, T., Grégoire, C., Espallergues, J., 2006. Neuro (active) steroids actions at the neuromodulatory sigma 1 (σ 1) receptor: biochemical and physiological evidences, consequences in neuroprotection. Pharmacol. Biochem. Behav. 84, 581–597.
Maurice, T., Strehaiano, M., Duhr, F., Chevallier, N., 2018. Amyloid toxicity is enhanced after pharmacological or genetic invalidation of the σ1 receptor. Behav. Brain Res. 339, 1–10.
Mavlyutov, T.A., Nickells, R.W., Guo, L.-W., 2011. Accelerated retinal ganglion cell death in mice deficient in the Sigma-1 receptor. Mol. Vision 17, 1034.
Mavlyutov, T.A., Epstein, M.L., Verbny, Y.I., Huerta, M.S., Zaitoun, I., Ziskind-Conhaim, L., Ruoho, A.E., 2013. Lack of sigma-1 receptor exacerbates ALS progression in mice. Neuroscience 240, 129–134.
Meunier, J., Hayashi, T., 2010. Sigma-1 receptors regulate Bcl-2 expression by reactive oxygen species-dependent transcriptional regulation of nuclear factor κB. J. Pharmacol. Exp. Ther. 332, 388–397.
Meunier, J., Ieni, J., Maurice, T., 2006. The anti-amnesic and neuroprotective effects of donepezil against amyloid beta25-35 peptide-induced toxicity in mice involve an interaction with the sigma1 receptor. Br. J. Pharmacol. 149, 998–1012.
Meurs, A., Clinckers, R., Ebinger, G., Michotte, Y., Smolders, I., 2007. Sigma 1 receptor-mediated increase in hippocampal extracellular dopamine contributes to the mechanism of the anticonvulsant action of neuropeptide Y. Eur. J. Neurosci. 26, 3079–3092.
Mishina, M., Ohyama, M., Ishii, K., Kitamura, S., Kimura, Y., Oda, K., Kawamura, K., Sasaki, T., Kobayashi, S., Katayama, Y., Ishiwata, K., 2008. Low density of sigma1 receptors in early Alzheimer's disease. Ann. Nucl. Med. 22, 151–156.
Monnet, F.P., Debonnel, G., Junien, J.-L., De Montigny, C., 1990. N-methyl-D-aspartate-induced neuronal activation is selectively modulated by σ receptors. Eur. J. Pharmacol. 179, 441–445.
Monnet, F.P., Mahé, V., Robel, P., Baulieu, E.-E., 1995. Neurosteroids, via sigma receptors, modulate the [3H] norepinephrine release evoked by N-methyl-D-aspartate in the rat hippocampus. Proc. Natl. Acad. Sci. 92, 3774–3778.
Moriguchi, S., Shinoda, Y., Yamamoto, Y., Sasaki, Y., Miyajima, K., Tagashira, H., Fukunaga, K., 2013. Stimulation of the sigma-1 receptor by DHEA enhances synaptic efficacy and neurogenesis in the hippocampal dentate gyrus of olfactory bulbectomized mice. PLoS One 8, e60863.
Morris, R., Anderson, E., Lynch, G.a., Baudry, M., 1986. Selective impairment of learning and blockade of long-term potentiation by an N-methyl-D-aspartate receptor antagonist, AP5. Nature 319, 774–776.
Nakazawa, M., Matsuno, K., Mita, S., 1998. Activation of σ 1 receptor subtype leads to neuroprotection in the rat primary neuronal cultures. Neurochem. Int. 32, 337–343.
Nelson, O., Tu, H., Lei, T., Bentahir, M., de Strooper, B., Bezprozvanny, I., 2007. Familial Alzheimer disease-linked mutations specifically disrupt Ca2+ leak function of presenilin 1. J. Clin. Invest. 117, 1230–1239.
Nilsson, M., Carlsson, A., Markinhuhta, K.R., Sonesson, C., Pettersson, F., Gullme, M., Carlsson, M.L., 2004. The dopaminergic stabiliser ACR16 counteracts the behavioural primitivization induced by the NMDA receptor antagonist MK-801 in mice: implications for cognition. Prog. Neuro-Psychopharmacol. Biol. Psychiatry 28, 677–685.
Noguchi, J., Matsuzaki, M., Ellis-Davies, G.C., Kasai, H., 2005. Spine-neck geometry determines NMDA receptor-dependent Ca2+ signaling in dendrites. Neuron 46, 609–622.
Ono, Y., Tanaka, H., Takata, M., Nagahara, Y., Noda, Y., Tsuruma, K., Shimazawa, M., Hozumi, I., Hara, H., 2014. SA4503, a sigma-1 receptor agonist, suppresses motor neuron damage in in vitro and in vivo amyotrophic lateral sclerosis models. Neurosci. Lett. 559, 174–178.
Ortega-Roldan, J.L., Ossa, F., Amin, N.T., Schnell, J.R., 2015. Solution NMR studies reveal the location of the second transmembrane domain of the human sigma-1 receptor. FEBS Lett. 589, 659–665.
Pabba, M., Wong, A.Y., Ahlskog, N., Hristova, E., Biscaro, D., Nassrallah, W., Ngsee, J.K., Snyder, M., Beique, J.-C., Bergeron, R., 2014. NMDA receptors are upregulated and trafficked to the plasma membrane after sigma-1 receptor activation in the rat hippocampus. J. Neurosci. 34, 11325–11338.
Pchitskaya, E., Kraskovskaya, N., Chernyuk, D., Popugaeva, E., Zhang, H., Vlasova, O., Bezprozvanny, I., 2017. Stim2-Eb3 association and morphology of dendritic spines in hippocampal neurons. Sci. Rep. 7, 17625.
Platt, R.J., Chen, S., Zhou, Y., Yim, M.J., Swiech, L., Kempton, H.R., Dahlman, J.E., Parnas, O., Eisenhaure, T.M., Jovanovic, M., Graham, D.B., Jhunjhunwala, S., Heidenreich, M., Xavier, R.J., Langer, R., Anderson, D.G., Hacohen, N., Regev, A., Feng, G., Sharp, P.A., Zhang, F., 2014. CRISPR-Cas9 knockin mice for genome editing

and cancer modeling. Cell 159, 440–455.
Popugaeva, E., Pchitskaya, E., Speshilova, A., Alexandrov, S., Zhang, H., Vlasova, O., Bezprozvanny, I., 2015. STIM2 protects hippocampal mushroom spines from amyloid synaptotoxicity. Mol. Neurodegener. 10, 37.
Rammes, G., Hasenjager, A., Sroka-Saidi, K., Deussing, J.M., Parsons, C.G., 2011. Therapeutic significance of NR2B-containing NMDA receptors and mGluR5 metabotropic glutamate receptors in mediating the synaptotoxic effects of beta-amyloid oligomers on long-term potentiation (LTP) in murine hippocampal slices. Neuropharmacology 60, 982–990.
Rammes, G., Gravius, A., Ruitenberg, M., Wegener, N., Chambon, C., Sroka-Saidi, K., Jeggo, R., Staniaszek, L., Spanswick, D., O'Hare, E., Palmer, P., Kim, E.M., Bywalez, W., Egger, V., Parsons, C.G., 2015. MRZ-99030 - a novel modulator of Abeta aggregation: II - Reversal of Abeta oligomer-induced deficits in long-term potentiation (LTP) and cognitive performance in rats and mice. Neuropharmacology 92, 170–182.
Rammes, G., Seeser, F., Mattusch, K., Zhu, K., Haas, L., Kummer, M., Heneka, M., Herms, J., Parsons, C.G., 2018. The NMDA receptor antagonist Radiprodil reverses the synaptotoxic effects of different amyloid-beta (Aβ) species on long-term potentiation (LTP). Neuropharmacology 140, 184–192.
Rodriguez, A., Ehlenberger, D.B., Dickstein, D.L., Hof, P.R., Wearne, S.L., 2008. Automated three-dimensional detection and shape classification of dendritic spines from fluorescence microscopy images. PLoS One 3, e1997.
Rung, J.P., Rung, E., Helgeson, L., Johansson, A.M., Svensson, K., Carlsson, A., Carlsson, M.L., 2008. Effects of (−)-OSU6162 and ACR16 on motor activity in rats, indicating a unique mechanism of dopaminergic stabilization. J. Neural Transm. 115, 899–908.
Ruscher, K., Shamloo, M., Rickhag, M., Ladunga, I., Soriano, L., Gisselsson, L., Toresson, H., Ruslim-Litrus, L., Oksenberg, D., Urfer, R., 2011. The sigma-1 receptor enhances brain plasticity and functional recovery after experimental stroke. Brain 134, 732–746.
Ryskamp, D.A., Popugaeva, E., Bezprozvanny, I., 2016. Calcium Hypothesis of Neurodegeneration. In: Neurodegenerative Diseases: Unifying Principles. Vol. 27.
Ryskamp, D., Wu, J., Geva, M., Kusko, R., Grossman, I., Hayden, M., Bezprozvanny, I., 2017. The sigma-1 receptor mediates the beneficial effects of pridopidine in a mouse model of Huntington disease. Neurobiol. Dis. 97, 46–59.
Sahlholm, K., Arhem, P., Fuxe, K., Marcellino, D., 2013. The dopamine stabilizers ACR16 and (−)-OSU6162 display nanomolar affinities at the sigma-1 receptor. Mol. Psychiatry 18, 12–14.
Sahlholm, K., Sijbesma, J.W., Maas, B., Kwizera, C., Marcellino, D., Ramakrishnan, N.K., Dierckx, R.A., Elsinga, P.H., van Waarde, A., 2015. Pridopidine selectively occupies sigma-1 rather than dopamine D2 receptors at behaviorally active doses. Psychopharmacology 232, 3443–3453.
Saito, T., Matsuba, Y., Mihira, N., Takano, J., Nilsson, P., Itohara, S., Iwata, N., Saido, T.C., 2014. Single App knock-in mouse models of Alzheimer's disease. Nat. Neurosci. 17, 661–663.
Sanjana, N.E., Shalem, O., Zhang, F., 2014. Improved vectors and genome-wide libraries for CRISPR screening. Nat. Methods 11, 783–784.
Saunders, A.M., Strittmatter, W.J., Schmechel, D., George-Hyslop, P.H., Pericak-Vance, M.A., Joo, S.H., Rosi, B.L., Gusella, J.F., Crapper-MacLachlan, D.R., Alberts, M.J., et al., 1993. Association of apolipoprotein E allele epsilon 4 with late-onset familial and sporadic Alzheimer's disease. Neurology 43, 1467–1472.
Schmidt, H.R., Zheng, S., Gurpinar, E., Koehl, A., Manglik, A., Kruse, A.C., 2016. Crystal structure of the human sigma1 receptor. Nature 532, 527–530.
Selkoe, D.J., 2002. Alzheimer's disease is a synaptic failure. Science 298, 789–791.
Smith, S.B., Duplantier, J., Dun, Y., Mysona, B., Roon, P., Martin, P.M., Ganapathy, V., 2008. In vivo protection against retinal neurodegeneration by sigma receptor 1 ligand (+)-pentazocine. Invest. Ophthalmol. Visual Sci. 49, 4154–4161.
Snyder, M.A., McCann, K., Lalande, M.J., Thivierge, J.P., Bergeron, R., 2016. Sigma receptor type 1 knockout mice show a mild deficit in plasticity but no significant change in synaptic transmission in the CA 1 region of the hippocampus. J. Neurochem. 138, 700–709.
Squitieri, F., Di Pardo, A., Favellato, M., Amico, E., Maglione, V., Frati, L., 2015. Pridopidine, a dopamine stabilizer, improves motor performance and shows neuroprotective effects in Huntington disease R6/2 mouse model. J. Cell. Mol. Med. 19, 2540–2548.
Srivats, S., Balasuriya, D., Pasche, M., Vistal, G., Edwardson, J.M., Taylor, C.W., Murrell-Lagnado, R.D., 2016. Sigma1 receptors inhibit store-operated Ca2+ entry by attenuating coupling of STIM1 to Orai1. J. Cell Biol. 213, 65–79.
Su, T.P., Hayashi, T., Maurice, T., Buch, S., Ruoho, A.E., 2010. The sigma-1 receptor chaperone as an inter-organelle signaling modulator. Trends Pharmacol. Sci. 31, 557–566.
Sun, X., Beglopoulos, V., Mattson, M.P., Shen, J., 2005. Hippocampal spatial memory impairments caused by the familial Alzheimer's disease-linked presenilin 1 M146V mutation. Neurodegener. Dis. 2, 6–15.
Sun, S., Zhang, H., Liu, J., Popugaeva, E., Xu, N.J., Feske, S., White, C.L., Bezprozvanny, I., 2014. Reduced synaptic STIM2 expression and impaired store-operated calcium entry cause destabilization of mature spines in mutant presenilin mice. Neuron 82, 79–93.
Tackenberg, C., Ghori, A., Brandt, R., 2009. Thin, stubby or mushroom: spine pathology in Alzheimer's disease. Curr. Alzheimer Res. 6, 261–268.
Tada, T., Sheng, M., 2006. Molecular mechanisms of dendritic spine morphogenesis. Curr. Opin. Neurobiol. 16, 95–101.
Takebayashi, M., Hayashi, T., Su, T.-P., 2004. A perspective on the new mechanism of antidepressants: neuritogenesis through sigma-1 receptors. Pharmacopsychiatry 37, 208–213.
Tang, T.S., Tu, H., Chan, E.Y., Maximov, A., Wang, Z., Wellington, C.L., Hayden, M.R., Bezprozvanny, I., 2003. Huntingtin and huntingtin-associated protein 1 influence neuronal calcium signaling mediated by inositol-(1,4,5) triphosphate receptor type 1. Neuron 39, 227–239.
Tsai, S.Y., Hayashi, T., Harvey, B.K., Wang, Y., Wu, W.W., Shen, R.F., Zhang, Y., Becker, K.G., Hoffer, B.J., Su, T.P., 2009. Sigma-1 receptors regulate hippocampal dendritic spine formation via a free radical-sensitive mechanism involving Rac1xGTP pathway. Proc. Natl. Acad. Sci. U. S. A. 106, 22468–22473.
Tsai, S.Y., Rothman, R.K., Su, T.P., 2012. Insights into the Sigma-1 receptor chaperone's cellular functions: a microarray report. Synapse 66, 42–51.
Tsai, S.Y., Pokrass, M.J., Klauer, N.R., Nohara, H., Su, T.P., 2015. Sigma-1 receptor regulates Tau phosphorylation and axon extension by shaping p35 turnover via myristic acid. Proc. Natl. Acad. Sci. U. S. A. 112, 6742–6747.
Tu, H., Nelson, O., Bezprozvanny, A., Wang, Z., Lee, S.-F., Hao, Y.H., Serneels, L., De Strooper, B., Yu, G., Bezprozvanny, I., 2006a. Presenilins form ER calcium leak channels, a function disrupted by mutations linked to familial Alzheimer's disease. Cell 126, 981–993.
Tu, H., Nelson, O., Bezprozvanny, A., Wang, Z., Lee, S.F., Hao, Y.H., Serneels, L., De Strooper, B., Yu, G., Bezprozvanny, I., 2006b. Presenilins form ER Ca2+ leak channels, a function disrupted by familial Alzheimer's disease-linked mutations. Cell 126, 981–993.
Uchida, N., Ujike, H., Tanaka, Y., Sakai, A., Yamamoto, M., Fujisawa, Y., Kanzaki, A., Kuroda, S., 2005. A variant of the sigma receptor type-1 gene is a protective factor for Alzheimer disease. Am. J. Geriatr. Psychiatry 13, 1062–1066.
Van Cauwenberghe, C., Van Broeckhoven, C., Sleegers, K., 2016. The genetic landscape of Alzheimer disease: clinical implications and perspectives. Gene. Med. 18, 421.
Waters, S., Tedroff, J., Ponten, H., Klamer, D., Sonesson, C., Waters, N., 2018. Pridopidine: Overview of Pharmacology and Rationale for its use in Huntington's Disease. J. Huntington's Dis. 7, 1–16.
Wu, J., Shih, H.P., Vigont, V., Hrdlicka, L., Diggins, L., Singh, C., Mahoney, M., Chesworth, R., Shapiro, G., Zimina, O., Chen, X., Wu, Q., Glushankova, L., Ahlijanian, M., Koenig, G., Mozhayeva, G.N., Kaznacheyeva, E., Bezprozvanny, I., 2011. Neuronal store-operated calcium entry pathway as a novel therapeutic target for Huntington's disease treatment. Chem. Biol. 18, 777–793.
Wu, J., Ryskamp, D.A., Liang, X., Egorova, P., Zakharova, O., Hung, G., Bezprozvanny, I., 2016. Enhanced store-operated calcium entry leads to striatal synaptic loss in a Huntington's disease mouse model. J. Neurosci. 36, 125–141.
Wu, J., Ryskamp, D., Birnbaumer, L., Bezprozvanny, I., 2018. Inhibition of TRPC1-dependent store-operated calcium entry improves synaptic stability and motor performance in a mouse model of Huntington's disease. J. Huntington's Dis. 7, 35–50.
Zhang, H., Sun, S., Herreman, A., De Strooper, B., Bezprozvanny, I., 2010. Role of presenilins in neuronal calcium homeostasis. J. Neurosci. 30, 8566–8580.
Zhang, H., Wu, L., Pchitskaya, E., Zakharova, O., Saito, T., Saido, T., Bezprozvanny, I., 2015. Neuronal store-operated calcium entry and mushroom spine loss in amyloid precursor protein knock-in mouse model of Alzheimer's disease. J. Neurosci. 35, 13275–13286.
Zhang, H., Sun, S., Wu, L., Pchitskaya, E., Zakharova, O., Fon Tacer, K., Bezprozvanny, I., 2016. Store-Operated Calcium Channel complex in Postsynaptic Spines: a New Therapeutic Target for Alzheimer's Disease Treatment. J. Neurosci. 36, 11837–11850.